Trends in Analytical Chemistry 180 (2024) 117948

Contents lists available at ScienceDirect

Trends in Analytical Chemistry

journal homepage: www.elsevier.com/locate/trac

Recent advances and trends in optical devices and sensors for hydrogen peroxide detection

John J. Galligan, Antje J. Baeumner, Axel Duerkop *

Institute of Analytical Chemistry, Chemo- and Biosensors University of Regensburg, Germany

ARTICLE INFO

Keywords:
H_2O_2
Hydrogen peroxide
Optical detection
Optical sensors
Single-use devices
HRP
Enzyme mimic
Smartphones

ABSTRACT

Hydrogen peroxide (H_2O_2) is a critically important, vital biomarker and hence a highly relevant analyte in a broad range of bioanalytical applications. The most recent trends furthering the ability of its reliable, reproducible, and sensitive quantification include the development of non-biological enzyme mimics, the investigation of smartphone cameras as transducers and detectors, and the continued development of semi-reversible and reversible detection strategies. While the non-biological catalysts offer stability-related advantages over enzymes while providing equally good limits of detection, critical questions regarding toxicity, persistence, (bio)accumulation, and overall environmental footprint need to be answered. In the case of heavy metal-based strategies a replacement by non-toxic, renewable alternatives should be an obvious research need. Signal recording has seen a dramatic change toward smartphones, with their ever-improving computing and image-acquisition abilities. Yet, with the sheer number of different camera and phone models progress can be difficult to assess, as reproducibility and comparability of results and experimental set-ups are too often elusive. In the area of semi-reversible sensors flow injection analysis (FIA) coupled with chemiluminescence (CL) remains the most advanced system. In the case of fully reversible sensors, research points toward oxygen-based sensing to be the most reliable. Analyzing publications from 2018 to 2024, it is not surprising that the important analytical figures of merit of low limits of detection (LODs), broad quantitation ranges, faster response and regeneration times combined with novel (reversible) probes continue to be and should remain central focus of future developments.

1. Introduction

Hydrogen peroxide (H_2O_2) plays a significant role in numerous physiological processes including, metabolic functions, apoptosis [1], cell-signaling [2] and immune-cell activation [3–5]. Its significance as an indicator of oxidative stress [6], a defence mechanism, and a contributor to aging is well-established [7,8]. It serves as a vital biomarker for various diseases, such as diabetes [9], cancer and has potential to be used in treatment of the latter [10], Parkinson's [11], cardiovascular diseases [12], Alzheimer's [13], and neurodegenerative disorders [14]. In food safety and quality, H_2O_2 is an important analyte, due to its use as food adulterant for example in milk, in many cases above allowed and thus potentially harmful concentrations [15].

The quantitation of H_2O_2 may be combined with oxidases of the large group of H_2O_2-producing enzymes, such as glucose, cholesterol, lactate, and glutamate oxidases, or with catalase as a H_2O_2-degrading enzyme. These coupled reactions allow for the development of sensors and bioassays that rely on H_2O_2 detection to quantify both enzyme substrates or products, thus widening the scope of probes for H_2O_2 [16–18]. Consequently, the ongoing research in (bio)sensors based on the detection for H_2O_2 has found applications and is of interest in fields including medical diagnostics [19], clinical research, food chemistry [20] and environmental investigations [21]. Furthermore, with the increasing use of peroxide-based explosives, such as triacetone peroxide in terrorist attacks, H_2O_2 as a residual precursor and indicator has unfortunately also become an important analyte to ensure the safety of first responders and security personnel [22].

Electrochemical and optical methods are the two major techniques broadly used for analysis and quantification of H_2O_2. Electrochemical devices are more frequently developed, more commonly published, usually offer fast response times and are in principle also applicable to continuous monitoring. The interfering challenges caused by other electroactive species present in various matrices at higher concentrations, such as vitamin C or uric acid, have long been solved by using a second redox reagent that is oxidized by H_2O_2 acting as a mediator or by using electrodes with selectively active or catalytic electrode surfaces

* Corresponding author.
E-mail address: axel.duerkop@ur.de (A. Duerkop).

https://doi.org/10.1016/j.trac.2024.117948
Received 11 March 2024; Received in revised form 25 July 2024; Accepted 1 September 2024
Available online 3 September 2024

and materials that can then detect specifically H_2O_2 at lower potentials [20]. Especially interesting is the development of reversible electrochemical systems [23]. Yet, electrode fouling is a serious issue not to be underestimated in real samples.

Optical H_2O_2 detection and quantification is often performed with commercially available assay kits, such as the colorimetric 3,3′,5,5′-Tetramethylbenzidin (TMB)/HRP or the fluorometric Amplex Red/HRP-assay. However, these assays require several preparation steps with buffer addition, and calibration via dilution series thus increasing assay time and the chance for erroneous data due to human error. Furthermore, sample preparation can require further steps as the dye and the enzyme have to be stored separately and at different temperatures, as it is the case for the Amplex Red assay. While the fluorescent and strongly pink reaction product resorufin that forms upon action of HRP or of other catalysts in presence of H_2O_2, is useful for both fluorometric [24] and colorimetric [25] detection, its applicability is limited due to an autocatalytic degradation of Amplex Red to resorufin when exposed to light [26]. In the past, detection methods based on the interaction of nanomaterials [27] or peroxidase [28] with H_2O_2 and the resulting optical change have also been developed and successfully used.

It is hence not surprising, considering the importance of H_2O_2 detection and the limited optical detection strategies that over the last two decades, a true plethora of H_2O_2-sensitive photoluminescent probes has been developed [29], many of which are in the field of organoboron-based probes [30–32]. These innovative fluorescent probes are applied for assay development and more importantly for cellular imaging, The experimental utilization of these innovative fluorescent probes is typically applied to standard bioassays and more importantly for cellular imaging. Unfortunately, most of the probes show an irreversible reaction with H_2O_2, making them useless for continuous or reversible measurements, and are thus far from the ideal chemical sensor [33]. Yet, they are often referred to as sensors irrespective of the definition IUPAC definition given in 1991 [34] requiring both a receptor and a transducer.

In many application scenarios, simpler and cheaper single-use disposable devices are preferrable over expensive and complex sensors, especially in point-of-care settings where factors like cross-contamination or harsh conditions would affect results negatively. These devices offer easy and cost-effective diagnostic and quantification capabilities, reducing the need for complex laboratory equipment and potentially lowering healthcare costs, such as pregnancy, COVID or glucose tests. Much recent research focuses on developing single-use devices for H_2O_2, which, when combined with H_2O_2 generating enzymes, facilitate the quantification of various biomarkers on-site. At this point, such point-of-care devices complement traditional sensors for H_2O_2, offering simple and rapid determination methods, while the latter may be preferred for more demanding online quantitation requiring higher instrumental effort over an extended period of time.

An additional challenge researchers will commonly encounter for optical applications when working with complex (biological) media and samples such as whole blood is having to overcome opacity and autofluorescence. Furthermore, the presence of catalases (which, to add to the nuisance are of course not present in the same concentration in every person [35]) and other H_2O_2-degrading species make the quantification of H_2O_2 both time-sensitive and thus unreliable, which to some degree could explain the concentration discrepancy and range reported in literature [36].

This critical review provides insight into the trends of recent (2018 – mid 2024) optical sensing devices and sensors for the detection of H_2O_2 focusing on colorimetric, chemiluminescent, photoluminescent detection and surface plasmon resonance approaches. In analyzing the trends, the authors decided that papers exclusively reliant on liquid assays conducted within cuvettes and microtiter plates, or applications restricted solely to imaging or (surface enhanced) Raman spectroscopy, were deliberately excluded from the article, with the latter having been reviewed recently [37]. Instead, focus is on studies encompassing a broader spectrum of novel, innovative methodologies and applications, ensuring a more diverse and comprehensive examination of the subject matter. Based on our literature analysis and the IUPAC definition of sensors and their possible classifications [34] we have categorized applications and devices into three groups.

- Single-use sensors and systems featuring a non-reusable detection/sensing module, exemplified by paper-based devices.
- Intermediate sensors and semi-reversible systems, in accordance with the classification by Moβhammer et al. [36], encompassing devices and sensing applications capable of semi-continuous detection. This involves the consistent introduction of reagents, akin to flow injection analysis (FIA), or relying on reactions reversible by external factors such as light, temperature, addition of redox reagents, or potential cycling to facilitate the regeneration of sensing capability.
- Fully reversible sensors.

Herein, we highlight innovative devices and sensors employing novel (enzymatic and enzyme mimicking) enhancement strategies and materials, (smartphone) detection and (semi) reversible and continuous sensors.

2. Single-use sensors and systems for quantitation of H_2O_2

2.1. Novel (enzymatic) enhancement strategies and materials

2.1.1. Enzymatic detection

Detection of H_2O_2 with HRP as a catalyst/recognition element is a classical way of signal generation. The commercial availability of this reasonably inexpensive enzyme has resulted in an abundance of published protocols demonstrating its rapid reaction kinetics under mild reaction conditions ideal for biological and bioanalytical applications. Standard protein chemistry allows conjugation to various (bio)molecules, immobilization and its use as a signal enhancement strategy. However, similar to most enzymatic applications it is susceptible to inhibition by interferences. In the case of HRP, cyanide, azide, hydroxylamine, and some heavy metal ions are most known for reaction inhibition. Furthermore, a higher background signal due to non-specific enzymatic conversion in the absence of H_2O_2, a high pH-dependent activity, a poor stability when exposed to higher temperatures and organic solvents limit HRP's application and calls for more research [38].

In order to increase the stability of HRP and reduce the experimental assay complexity, some research focuses on the encapsulation or immobilization of HRP in a suitable matrix such as a polydimethylsiloxane (PDMS) layer with a GPT linker [39] (Table 1), in a carbon dot-doped hydrogel sensor array [40], as enzyme-inorganic nanoflowers made from EDTA, $CaHPO_4$ and HRP [41], gold nanoparticle(AuNP)-enzyme [42] or HRP-BSA AuNP nanoclusters [43]. The respective approaches hone in on providing a reusable and simple CL-platform by Bocanegra-Rodríguez et al. [39] to achieve an LOD of 0.02 $\mu mol \cdot L^{-1}$ range 0.06–10 $\mu mol \cdot L^{-1}$, a multiplexing, PDMS-housed sensing array for H_2O_2-mediated colorimetric detection of wound-related biomarkers such as glucose and uric acid and non-H_2O_2 mediated like pH, total protein and urea with good accuracy by Zheng et al. [40], enabling colorimetric H_2O_2 detection with TMB was developed by Tian et al. whose nanoflowers maintained 90 % activity over 30 days at −20 °C, offering potential in applications like prostate cancer screening and water quality monitoring and achieving an LOD of 1 $\mu mol \cdot L^{-1}$ and an analytical range of 2–100 $\mu mol \cdot L^{-1}$ [41], integration of luminescent HRP-Au nanoclusters into a microfluidic droplet device for single-cell secreted H_2O_2 detection by Shen et al. [42] or the encapsulation of advanced HRP-BSA AuNP nanoclusters [43] into a glass-based microfluidic device limited to visual detection and an LOD of 0.5 $nmol \cdot L^{-1}$ and a reasonably broad analytical range of 0.5–50 $nmol \cdot L^{-1}$ in

Table 1
Single-use sensors and systems for the detection of H_2O_2 presented in this review. LODs and ranges in italics represent data collected in ideal laboratory conditions such as cuvette measurements in a cuvette spectrometer and not in the proposed sensor design, the latter are given in non-italics. Excitation and emission wavelengths given are either the used wavelengths in the publication or the respective excitation/emission maxima of the respective dye(s) (the latter is indicated by a *). For colorimetric measurements the maximum absorbance wavelength is given. For CL measurements the detection wavelength of the emission in the publication is given.[a]: only visual quantification.

Probe/recognition element	Detected signal	$\Lambda_{exc}/_{em}$	Device type	(LOD) Analytical Range of H_2O_2	Real world sample type	Comments	Ref
Enzymatic detection							
Luminol/HRP	HRP/Luminol chemiluminescence	424*	Reaction tube	(0.03 μmol·L^{-1}) 0.06–10 μmol L^{-1}		Reusable	[39]
Amplex Red/HRP	HRP/H_2O_2 oxidation of Amplex Red to resorufin	572*	colorimetric readout with a smartphone, cellulose based carrier material	(3.4 μmol·L^{-1}) 10–100 μmol·L^{-1}	Histamine and tyramine in PBS, tuna sample	For simultaneous detection of histamine and tyramine	[25]
ABTS, 4-Aminoantipyrene/ HRP	Colorimetric oxidation of ABTS and 4-Aminoantipyrene	415, 510*	Colorimetric readout with a smartphone, carbon dot doped hydrogel in microfluidic PDMS sensor array		pH, glucose, urea, uric acid and total protein from rat wound fluid		[40]
TMB/HRP	HRP catalyzed oxidation of TMB	652*	Paper-based smartphone readout	(1 μmol·L^{-1}) 2–100 μmol·L^{-1}	H_2O_2 in liquor and water	Can also detect salicylic acid	[41]
HRP-AuNCs	Luminescence quenching	542/620	Microfluidic	(1 nmol·L^{-1}) up to 40 nmol•L^{-1}	H_2O_2 secreted from single cells		[42]
Protein-stabilized gold nanoclusters HEFBNPs	Luminescence quenching	248/720	Microfluidic	*(500 pmol·L^{-1}) 500 pmol·L^{-1}* - 50 mmol·L^{-1}	River water	Microfluidic sensor only with visual readout	[43]
Layer-by-layer embedded AGNPs + AuNPs	LSPR		LSPR Flow Cell	(2.7 ppm)			[44]
Poly(aniline-co-anthranilic acid) (ANI-co-AA) composite film/HRP	Colorimetric change of composite film	655*	Film-based colorimetric readout with a smartphone	(*35.6 μmo·L^{-1}*, 51.2 μmol·L^{-1}) *25*–200 μmol·L^{-1}	H_2O_2, glucose and catechol in diluted juice samples	For simultaneous detection of H_2O_2, glucose and catechol	[45]
Guaiacol/HRP	Colorimetric change of Guaiacol to Tetraguaiacol		Paper-based	(0.354 mmol·L^{-1}) 1.25–15 mmol L^{-1}	H_2O_2 in Milk		[46]
Enzyme mimics and catalysis enhanced sensing							
TMB/Fe_3O_4 QD	Colorimetric oxidation of TMB	652	Capillary-based array	(4.5 μmol·L^{-1}) 10–100 μmol·L^{-1}	Milk		[53]
TPA/Cu(II)/Co(II) organic gel	Oxidation of TPA to 2-hydroxyTPA with Cu(II)/ Co(II) organic gel in presence of H_2O_2	315/446	Hydrogel-based	(81 nmol·L^{-1}) 0–120 μmol·L^{-1}	H_2O_2 and glucose in PBS (pH 7.0)	Metal-organic gel with peroxidase activity	[54]
Luminol/Guanosine/ hemin hydrogel	Chemiluminescence	424*	Smartphone readout of GOx-loaded guanosine/ hemin CL hydrogel cartridge	(7 μmol·L^{-1})	Glucose in artificial serum		[56]
TMB/$PtNi_3$	Colorimetric oxidation of TMB	652*	Paper-based with custom-made portable colorimeter	(0.03 μmol·L^{-1}) 0.1–10 μmol·L^{-1}	H_2O_2 sectreted from HELA cells	Fast 3 min assay speed. Catalyst/nanozyme also useable in electrochemical detection	[55]
TMB/sericin-modified silver nanozyme	Colorimetric oxidation of TMB	652*	Paper-based origami pad	(0.15 mg·dL^{-1}) 0.5–240.0 mg·dL^{-1}	H_2O_2 and Glucose in salvia		[57]
TMB/cellulose membranes with immobilized Au nanoclusters	Colorimetric oxidation of TMB	652*	Paper-based	(7 mmol·L^{-1}[a])			[58]
TMB/MoS_2–$SrTiO_3$ nanocomposite	Colorimetric oxidation of TMB	652*	Paper-based	(80 nmol·L^{-1}) 0.1–5 μmol·L^{-1}			[59]
TMB/MoS_2@$CoTiO_3$ nanocomposite	Colorimetric oxidation of TMB	652*	Paper-based	*(0.01 μmol·L^{-1})*	H_2O_2 in milk and tap water		[60]
TMB/Cellulose nanofibrils/Fe-doped carbon dot composite nanopapers	Colorimetric oxidation of TMB	652*	Paper-based with smartphone readout	(0.93 μmol·L^{-1}) 6–42 μmol·L^{-1}		Reusable enzyme mimic strips after cleaning/regeneration with ascorbic acid	[61]
TMB/Pd–Pt@hemin-rGO/CNTs-COOH	Colorimetric oxidation of TMB	652*	Paper-based	*(0.01 μmol·L^{-1})*			[62]
TMB/B, N, and S co-doped carbon dots (BNS-CDs) peroxidase mimic	Colorimetric oxidation of TMB	652*	Smartphone RGB readout	(0.8 μmol·L^{-1}) 3–30 μmol·L^{-1}	Moutwhash and milk		[63]
ABTS/MoOx QDs	Colorimetric oxidation of ABTS	420*	Paper-based	(0.175 μmol·L^{-1})	H_2O_2 released from PC12 cells		[64]

(*continued on next page*)

Table 1 (*continued*)

Probe/recognition element	Detected signal	$\Lambda_{exc}/_{em}$	Device type	(LOD) Analytical Range of H_2O_2	Real world sample type	Comments	Ref
TMB/CuO hollow sphere nanozyme	Colorimetric oxidation of TMB	652*	Paper-based	(2.1 μmol·L^{-1}) 2.4–150 μmol·L^{-1}			[65]
CPT-MnBG-Gel	Luminescence quenching	254/544	Hydrogel-based wound dressing	(10.35 μmol·L^{-1}) up to 200 μmol·L^{-1}	Diabetic wound	H_2O_2 scavenging for diabetic wound treatment	[69]
Carboxyluminol/Hemin	Chemiluminescence	430	μPAD based point-of care device for lactate readout with smartphone or CCD-camera	(13 μmol·L^{-1}) up to 2000 μmol·L^{-1}		Can also detect lactate	[71]
Luminol/$CoCl_2$	Chemiluminescence	424*	miniaturized 3D-printed device	(3.0·10^{-5} % (w/w) / 9 μmol·L^{-1}) 1.0·10^{-4} - 9.0·10^{-3} % (w/w) 30–270·μmol L^{-1}	H_2O_2 in milk		[72]
IR820 Core-shell UCNP	Inhibition of ET to UCNP by oxidation of IR820 with OH in Fenton-type reaction	808 + 980/ 525 + 540	Flow-cell based	(0.1 nmol·L^{-1}) 0.5–100 nmol·L^{-1}			[75]
Fe-based MOFs/OPD	Dual-mode ratiometric fluorescence quenching with colorimetric change	365/ 447 + 572 450	3D printed chip holder and chip with machine learning smartphone image evaluation	*2.06·nmol•L^{-1}*			[76]
Non-catalytic detection							
Tb^{3+}/Eu^{3+} [1,1′-Biphenyl]-4-carboxylic acid deboraontion	Ligand energy transfer luminescence	270/545 270/617	Hydrogel-drop-caoted paper discs	(2 μmol·L^{-1}) 2–200 μmol·L^{-1}	H_2O_2 in hand sanitizer		[77]
C6NIB deboronation	Fluorescence	458/522	Aluminum foil-based silica gel plate	2 ppb	H_2O_2 vapor	Very fast response time of <0.5 s for high concentrations of H_2O_2 possible	[78]
Pyrene/fluorene-based probes DB-WCZ DB-W deboronation	Fluorescence	370/449	Thin film	(2.2 ppb)	H_2O_2 vapor		[79]
HFPQ@ALB Deboronation	Ratiometric fluorescence	365/ 515 + 484	Paper-based/ miniaturized measurement chamber + smartphone readout	Up to 200 μmol·L^{-1} paper-based Up to 100 μmol·L^{-1} miniaturized chamber	H_2O_2 in milk		[80]
Maleimide-functionalized tetraphenylethene (TPE-M) and cysteine	Aggregation induced emission (AIE)/quenching	365/460	Paper-based	(2.5 μmol·L^{-1} paper-based 10 nmol·L^{-1} in solution) up to 20 μmol·L^{-1}	H_2O_2 and glucose in PBS (pH 7.0)		[81]
Cu nanoclusters with Ce^{3+}	AIE quenching	350/650	Paper based	(3 μmol·L^{-1}) 14–140 μmol·L^{-1}			[82]
Luminol	Ultrasonic/H_2O_2-induced SCL of luminol	424	Apertureless stainless steel substrate USB piezoelectric ultrasonic transducer	(0.32 μmol·L^{-1}) 0.5–50 μmol·L^{-1}	Glucose/GOx in PBS (pH 7.4)		[83]
Ag NPs-alginate composite	Colorimetric change	400	Paper-based with a smartphone readout	(0.1 mmol·L^{-1}) 0.1–10 mmol·L^{-1}		Photobox dimensions suitable for multiple smartphone models	[84]
PF-PDMTP/HQ	Fluorescence quenching	365/ 420 + 650	Paper-based with smartphone greyscale readout	(9.4 μmol·L^{-1}) up to 200 μmol·L^{-1}	Human salvia		[85]

cuvette-measurements (Fig. 1). However, for a better comparability of the performance in the cuvette and of the microfluidic device, a signal data acquisition of the HRP-encapsulated fluorescent bio-nanoparticles (HEFBNPs) beyond mere detection with eye-vision, especially considering the impressively low LOD and analytical range, would have been desirable.

Goicoechea et al. [44] developed a self-referenced optical fiber sensor for H_2O_2 detection based on localized surface plasmon resonance (LSPR) of metallic nanoparticles in layer-by-layer (LbL) films. The sensor utilizes a LbL nanoassembly technique to fabricate sensitive nanocoatings on the optical fiber core. The nanocoatings incorporate both silver nanoparticles (AgNPs) and gold nanoparticles (AuNPs), which exhibit different sensitivities to H_2O_2. The LOD of the sensor is estimated to be 2.7 ppm and allowed for compensation of light source fluctuations, sensor drift and measurements of a total of 40 min. Unfortunately, the signal from the LSPR absorption bands was noisy impacting signal quality, in the current setup, presumably due to dipping of the sensor into solutions, instead of using a flow-system, which would have been desirable. While the sensor did show no to very little signal change in presence of interferents such as Hanks' Balanced Salt Solution (HBSS), glucose and ascorbic acid, a measurement in a real 'live' cell culture or any other complex matrix to see the effect of cell matter and proteins on the sensor would have been interesting.

Main focus on paper-based colorimetric enzyme-based devices using HRP take advantage of smartphones for signal recording. For Galbán [25], Amplex Red provided significantly better LODs as demonstrated for the precise and reproducible detection of histamine/tyramine and H_2O_2 than using TMB or ABTS, as their approach avoids the issue of lateral reactions such as the oxidation of the dye by the aldehyde forming in the oxidation step of histamine. Yet, as indicated in the

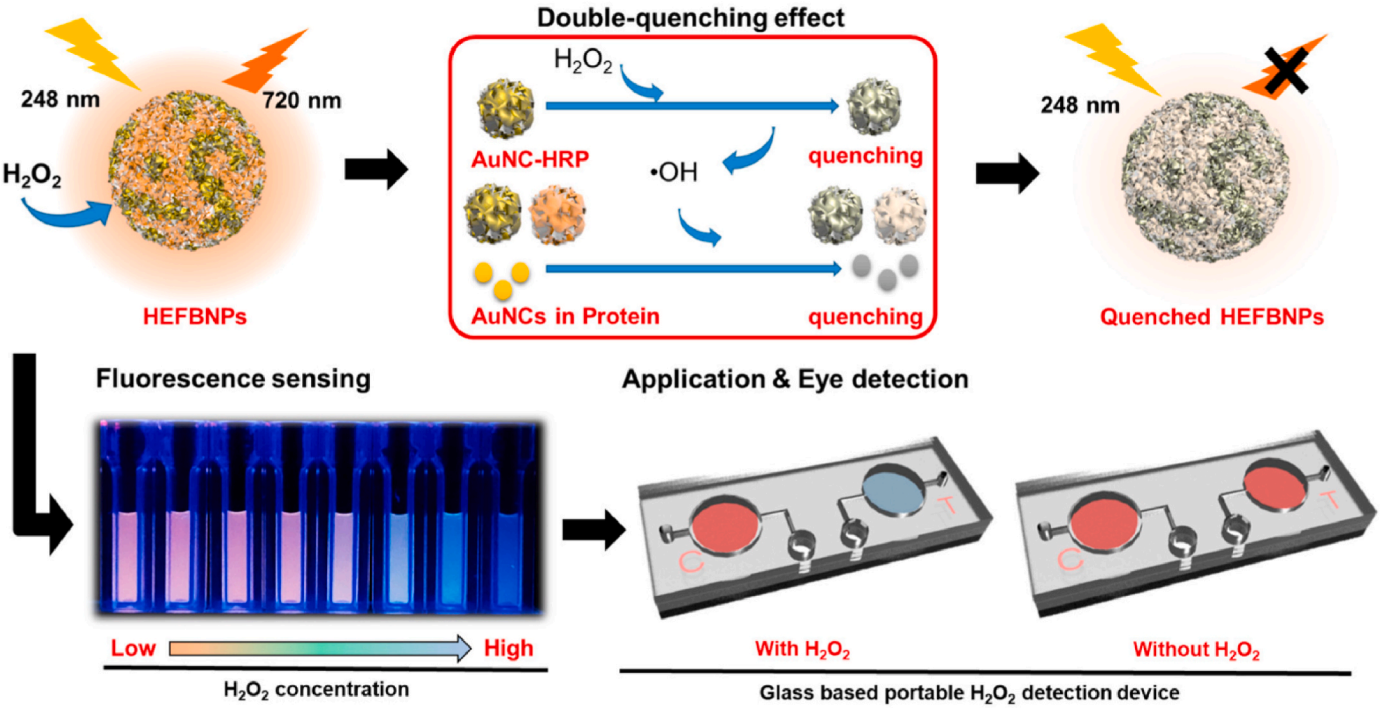

Fig. 1. Schematic illustration of the quenching mechanism of the innate Au-nanoclusters HEFBNPs fluorescence by addition of H_2O_2 and its applications. Reprinted with permission from Ref. [43]. ©MDPI.

introduction, both Amplex Red and the respective peroxide-generating enzymes require refrigeration for storage inhibiting the applicability in the field. In the case of Hosu et al. [45] a poly(aniline-co-anthranilic acid) (ANI-co-AA) composite film was used as substrate. It was applied in a multiplexing platform reaching LODs of 34.6 μmol·L^{-1} by spectrophotometric detection and 51 μmol·L^{-1} with the smartphone, thus not providing the most sensitive device, an acceptable trade-off for its simplicity in use, a 2 min assay time, the multiplexing assay and the accessibility of the smartphone readout. The advantage of the of the film material was, that it could not just act as carrier/immobilization membrane for the enzyme, but also as chromogenic reagent. Lima et al. [46] used guaiacol in a paper-based device with wax-printed wells together with self-extracted peroxidase from zucchini for the detection and quantification of H_2O_2 in milk. With a linear calibration between 1.25 mmol·L^{-1} and 15 mmol·L^{-1} they were able to achieve an LOD of 0.354 mmol·L^{-1} and an LOQ of 1.18 mmol·L^{-1} respectively. In spiked milk samples, they were able to achieve recovery values between 92.2 % and 108 % whilst maintaining relative standard deviations below 6.5 %. Guaiacol is hence an interesting substrate as it delivers appropriate detection limits while being much cheaper than other colorimetric substrates.

2.1.2. *Enzyme mimic-based and catalysis-enhanced sensing*

Synthetic enzyme mimics or nanozymes have proven to be a true gamechanger in the field of optical sensing of hydrogen peroxide. In the last 15 years, the development of synthetic materials with alleged peroxidase activity has been increasingly successful [47] with their use being reported in several electrochemical sensors [48]. Initial papers describe the use of Fe_3O_4-NPs and graphene derivatives. Currently, other nanomaterials dominate the research landscape. Such studies are e.g. based on the structural and surface modification of already existing mimics, of new metal organic frameworks (MOFs) including their surface activation/increase, and the search for more sustainable synthesis and precursors/educts. So called enzyme mimics or nanozymes are supposed to overcome issues such as storage and temperature stability, limitations of pH-dependent activity and can provide a tunable activity [49,50]. As with any nanomaterial, one of the major issues is the reproducibility of their synthesis, size, homogeneity, and batch-to-batch variations. Crucial questions regarding toxicity have to be addressed before moving to *in-vivo* or clinical applications. Of equal importance is the environmental impact where release into the environment is possible, a consideration that is unfortunately rather rare in literature.

Also in optical assay strategies these peroxidase-mimicking artificial enzymes are increasingly employed [51,52]. Major advances made over the last years include the development gel-based matrices with peroxidase-mimicking ability and the integration of novel synthetic enzyme surrogates in paper-based devices. In the first case, the list of such novel gel-based devices include, a capillary array-based colorimetric platform to detect H_2O_2 in milk with sodium alginate coated Fe_3O_4-NPs and TMB showing an enhanced catalytic activity [53] in comparison to 'naked' NPs, a Cu(II)/Co(II) bimetallic organic gel with enhanced peroxidase-like activity, requiring 20 min at 45 °C [54], a dual-use $PtNi_3$ hydrogel with high stability, selectivity and reproducibility as electrocatalyst for electrochemical and as peroxide-like nanozyme with TMB for the colorimetric detection of H_2O_2 secreted from HELA cells in a custom-made portable colorimetric sensor [55] or the development of a chemiluminescent glucose POC device with a peroxidase-like hemin containing guanosine hydrogel loaded with luminol in analytical cartridges for smartphone detection [56] (Fig. 2). In all of these assays the used mimics showed competitive catalytic activity in comparison to HRP or were able to provide catalytic activity in HRP-adverse conditions.

In the case of paper-based strategies, innovation afforded through an enzyme mimic is paired with the unique advantages of the simplistic, yet adaptable assay format. Listed here are a few especially interesting publications that have demonstrated applicability in real matrices in all cases. For example, sericin-capped AgNPs were integrated into a paper-based origami folding device whereby folding the paper-based device the sample flows through the enzyme layer (for the glucose device) or the enzyme mimic layer before reaching the TMB reagent (Fig. 3). This origami layout allowed for both, the separation of the reagents and catalysts/enzymes and showed improved assay speed in comparison to

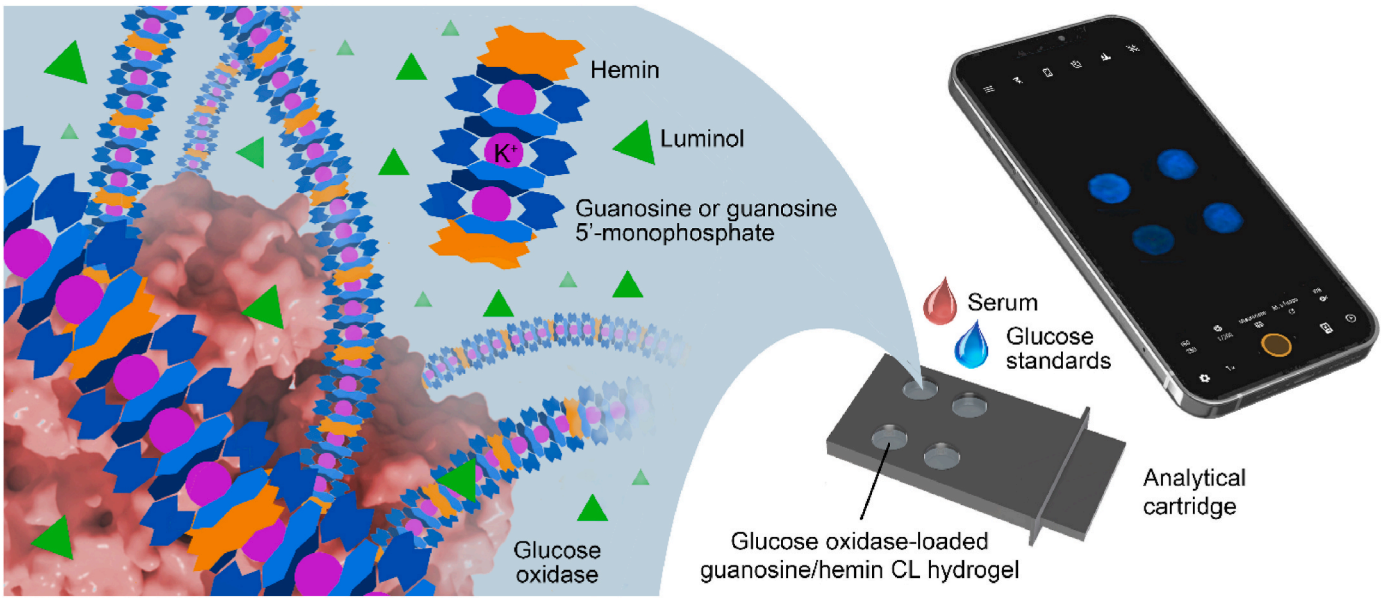

Fig. 2. Illustration of the peroxidase-mimicking G-quadruplex guanosine-derived hydrogel loaded in analytical cartridges for chemiluminescent detection of glucose and H_2O_2 for smartphone-based detection as developed by Calabria et al. Reprinted with permission from Ref. [56]. ©2023 MDPI.

'classical' paper-based devices [57]. Cheng et al. utilized mesoporous CuO hollow sphere nanozymes in a paper-based device for a smartphone-based readout [65] (Fig. 4). However, the authors fail to mention any specifics regarding lighting and camera settings and how the smartphone was held in position. Cellulose membranes with immobilized Au nanoclusters acting as peroxidase mimic for the detection of H_2O_2 and uric acid were proposed by Wei et al. [58]. Peroxidase-mimicking MoS_2–$SrTiO_3$ [59] and alginate-gel stabilized MoS_2@$CoTiO_3$ [60] nanocomposites for colorimetric detection of H_2O_2 with TMB were applied in paper-based formats. Research on cellulose nanofibrils/Fe-doped carbon dot composite nanopapers for the smartphone-based colorimetric detection of H_2O_2 and glucose was published by Bandi et al. [61]. Most notably, the group was able to recycle and reuse the test strips with the enzyme mimic with treatment of 0.1 mol·L^{-1} ascorbic acid, followed by washing steps up to 10 times without a significant loss of activity. The group of Qui [62] used self-assembled nanocomposite Pd–Pt@hemin-rGO/CNTs-COOH in paper-based indicator strips with TMB for the detection of H_2O_2. Beng et al. synthesized carbon dots co-doped with B, N, and S for smartphone-based colorimetric detection of H_2O_2 in samples like milk and mouthwash [63]. Another group [64] used molybdenum oxide quantum dots (MoOx QDs) showing peroxidase-like activity on a microfluidic paper-based analytical device for the rapid colorimetric detection of H_2O_2 released from PC12 cells with ABTS as dye. The paper-based device was able to detect H_2O_2 with an LOD of 0.175 µmol·L^{-1} after an assay time of 10 min.

Overall enzyme mimics can provide an innovative and intriguing alternative to classical enzymatic catalysis in H_2O_2 detection. Aside from the general limitations and issues aforementioned, it is crucial to see more benchmark experiments with HRP in place of the mimic. Only this would allow for true comparability and as proof of an actual improvement or advantage of the mimics over the enzyme. Few researchers spend time and resources on such often enough tedious comparison studies since assay parameters for enzymes and mimics differ. Thus, such parameter misalignment when done poorly, will potentially compromise comparability once more. Furthermore, the terms or rather neologisms nanozyme and enzyme mimics are often coined to new catalysts with improved surface structures or combinations of metals employed in reactions that result in the same detectable product as with an enzymatic reaction, i.e. TMB in a Fenton-type reaction without the peroxidase-typical two-electron process. Often Michaelis-Menten kinetics for single-enzyme, single-substrate [66] systems are used despite the often-encountered two-substrate mechanism [53] where other kinetic models, such as Langmuir-Hinselwood [67] are better suited to describe the observed reaction time course. Furthermore, a sufficient saturation with substrate or the amount of catalytically active surface or centers in comparison to the used weight is often ignored. That raises the question if the employed substances qualify for the term nanozyme or enzyme mimic and, if needed in excessive amounts 600 µg·mL^{-1} of Fe_3O_4 QDs vs 500 µg·mL^{-1} TMB [53], even as a catalyst or just as a stochiometric reagent [68].

In the field of catalytically enhanced H_2O_2-sensing, next-generation probes have provided much advancement in the detection of H_2O_2. Huang et al. developed a biocompatible GelMA hydrogel with encapsulated Mn-containing bioactive glass and $CePO_4$:Tb (CPT-MnBG-Gel) for wound monitoring and H_2O_2 scavenging capabilities for faster wound healing [69]. Through chemical modification of luminol, *m*-carboxyluminol demonstrated an enhanced CL-signal [70] and was successfully integrated in µPADs with the option of a smartphone-based readout [71] where H_2O_2 was detectable with an LOD of 13 µmol·L^{-1} with a range of up to 2000 µmol·L^{-1} and lactate with an LOD of 0.03 mmol·L^{-1} with an analytical range of up to 100 mmol·L^{-1} (Fig. 5). The integration of previously known catalysts and reagents into paper-based or miniaturized 3D-printed devices are other innovations seen in literature. For chemiluminescent quantification of H_2O_2 in milk, featuring a dedicated variable gain amplification system, and disposable wells with a hydroxyethyl cellulose-based detection membrane, miniaturized 3D-printed devices with disposable cartridges and flow-systems were developed by Vasconelos et al. (Fig. 6) [72]. They allowed detection of H_2O_2 down to an LOD of 9 µmol·L^{-1} and a linear range of approximately 30–270 µmol·L^{-1}.

Upconverting nanoparticles (UCNPs) have shown to be a valuable approach to work with or in complex biological matrices. Here, the efficiency and reliability of traditional probes and sensors are often challenged by many interfering substances as well as physical, chemical, and biological barriers. UCNPs are nanoparticles based on a nanocrystalline host e.g., $NaYF_4$ or $LiYF_4$ that have the ability to convert low energy NIR light into visible light with higher energy by serial multiphoton excitation steps. The various (and complex) mechanisms of upconversion and the design and variety of upconverting nanoparticles

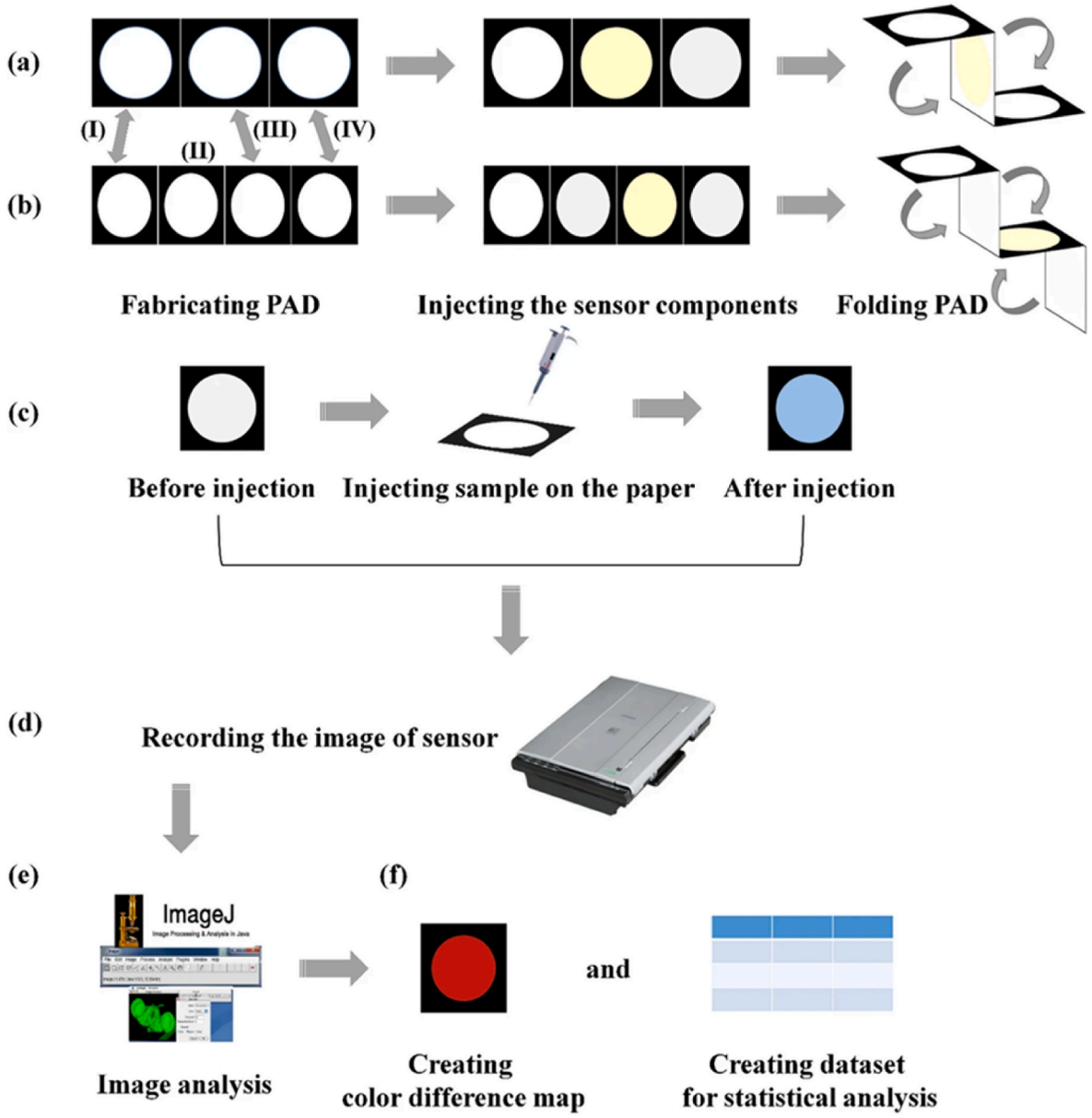

Fig. 3. Mirzaei et al. developed a paper-based origami folding device for the detection of glucose and H_2O_2. Layout and design of the devices for (**a**) H_2O_2 and (**b**) glucose detection. With (**I**) injection, (**II**) GOx (glucose-detection exclusive), (**III**) nanozyme and (**IV**) detection layer). (**c**) Assay procedure and colorimetric change. (**d**) Recording the image of sensor before and after exposing to analyte. (**e**) Image analysis in ImageJ, (**f**) evaluation of color difference map. Reprinted with permission from Ref. [57]. ©2023 Springer. (For interpretation of the references to colour in this figure legend, the reader is referred to the Web version of this article.)

are highly interesting and literally exciting topics that has been reviewed thoroughly elsewhere [73,74]. When doped with Yb^{3+} as sensitizer and Er^{3+} as acceptor, UCNPs have the capability to be excited close to the optical window of tissue allowing a deep tissue penetration. Moreover, UCNPs offer great optical properties among low auto-fluorescence, high signal-to-noise ratios, exceptional photostability and non-blinking emission. Despite some issues with UCNPs such as the susceptibility to water quenching and the significantly lower quantum yield and overall brightness in comparison to organic dyes, UCNPs have become an increasingly popular choice and powerful tool for photodynamic therapy approaches as well as sensor and probe development [73,74]. Their applicability for H_2O_2 detection was beautifully demonstrated by Wang et al.'s [75] device with an integrated pump for long-term monitoring of H_2O_2 in ovarian cancer peritoneal metastasis (Fig. 7). Good sensitivity and real-time detection capabilities show promise, yet challenges remain regarding *in-vivo* applicability and long-term stability. Unfortunately, the device is being hamstrung by its detection method with the irreversible oxidation of the used IR820 dye by •OH produced in a Fenton-type reaction, making replacement of the sensing membrane necessary for longer measurements underscoring the need for further research and refinement in this field.

Wu et al. [76] developed a portable dual mode sensing chip combined containing *o*-phenylenediamine (OPD) as colorimetric reagent together with facet-engineered iron-based MOFs as enhanced Fenton-type catalysts and fluorometric agents (Fig. 8). In their chip the sample would first be exposed to the MOFs producing •OH and quenching the MOF fluorescence with a simultaneous emission color shift from blue to yellow. The produced •OH could then be washed to the second pad containing OPD resulting in a colorimetric change. This change in MOF emission and dye color change could be captured with a

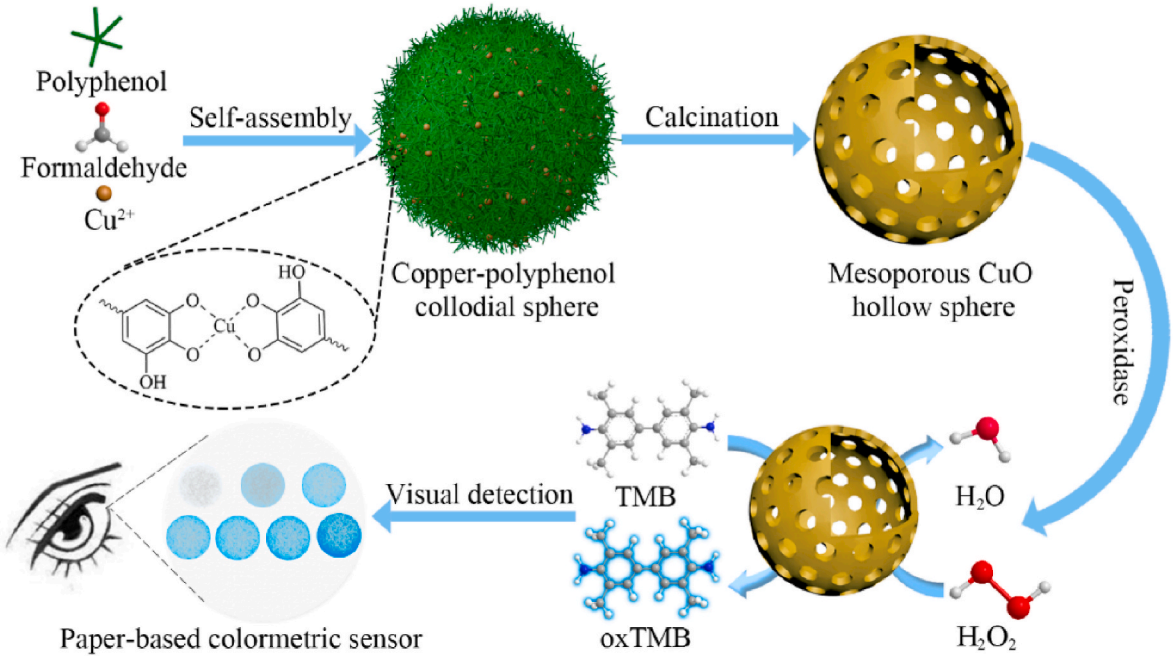

Fig. 4. Cheng et al. developed a paper-based platform with mesoporous CuO hollow sphere nanozymes as peroxidase mimic for the colorimetric detection of H_2O_2. Reprinted with permission from Ref. [65]. ©2021 MDPI.

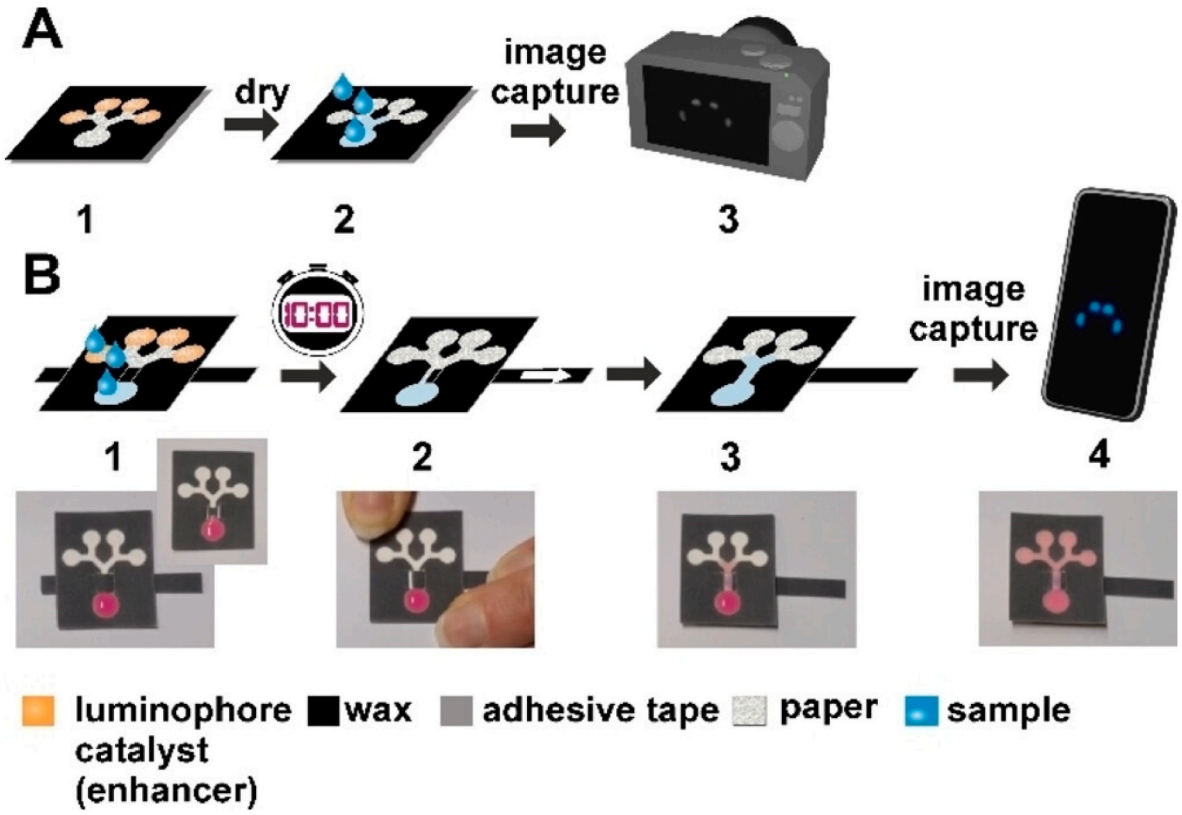

Fig. 5. Rink et al. present a wax-printed μPAD with the enhanced CL-reagent carboxyluminol for the smartphone- or CCD-camera-based detection of H_2O_2. Stepwise illustration of the assay procedure in (A) for H_2O_2 detection and luminophore detection with (1) applying sample to sample zone, (2) signal development and (3) taking images with a CCD camera and in (B) for the L-lactate assay with (1) applying sample to sample zone, incubation for 10 min, (2) opening sample chamber (3) signal development and (4) taking images with either a smartphone or CCD camera, schematic illustration, and real images with sulforhodamine B dye solution for better illustration of liquid flow. Reprinted with permission from Ref. [71]. ©Wiley 2023.

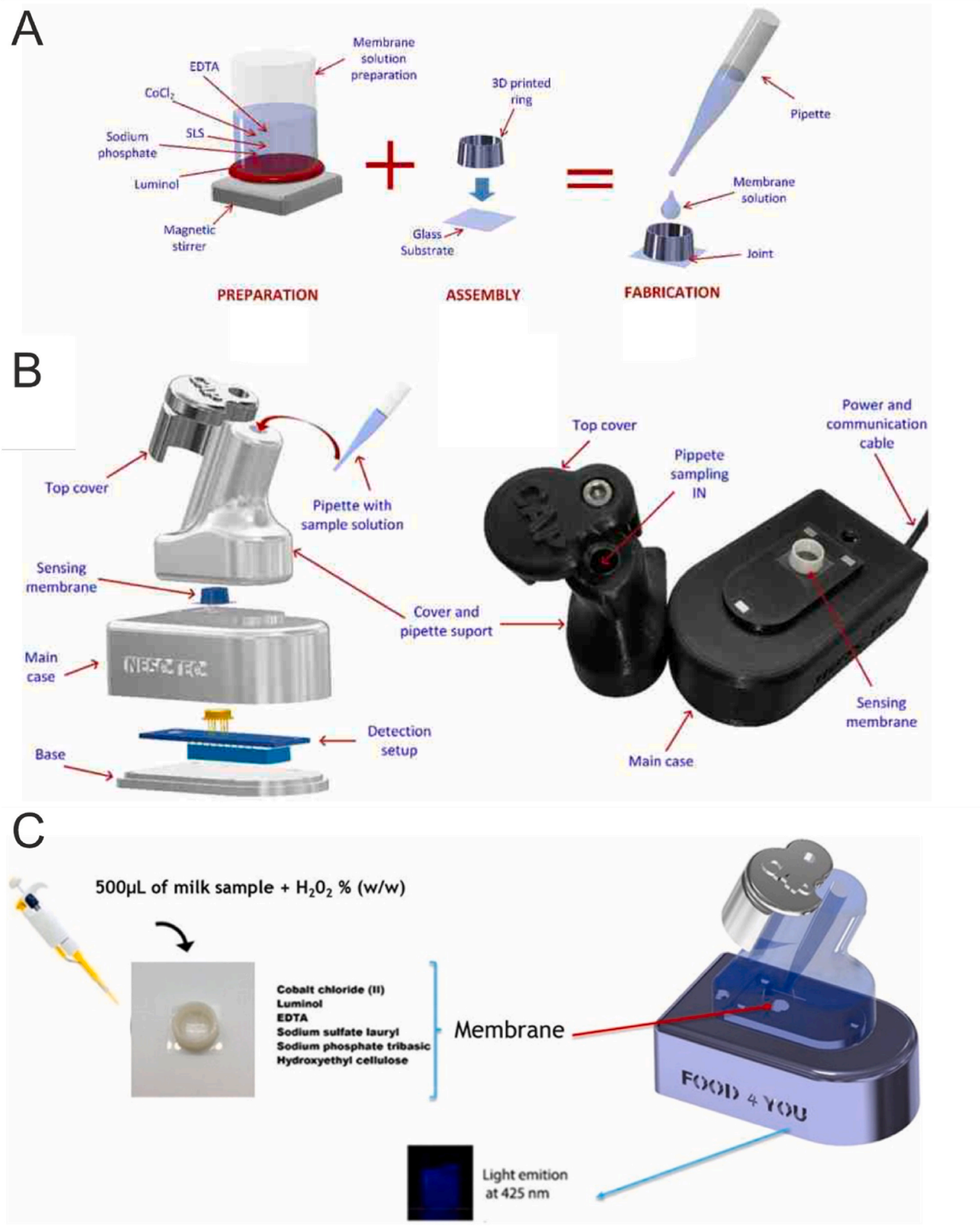

Fig. 6. A miniaturized 3D-printed device for chemiluminescent quantification of H_2O_2 in milk developed by Vasconelos et al. A) Scheme of the sensing membrane fabrication; B) Exploded view of the integrated detection module. C) Image of the sensing module and chemiluminescence at 425 nm. Reprinted with permission from Ref. [72]. © 2023 Elsevier.

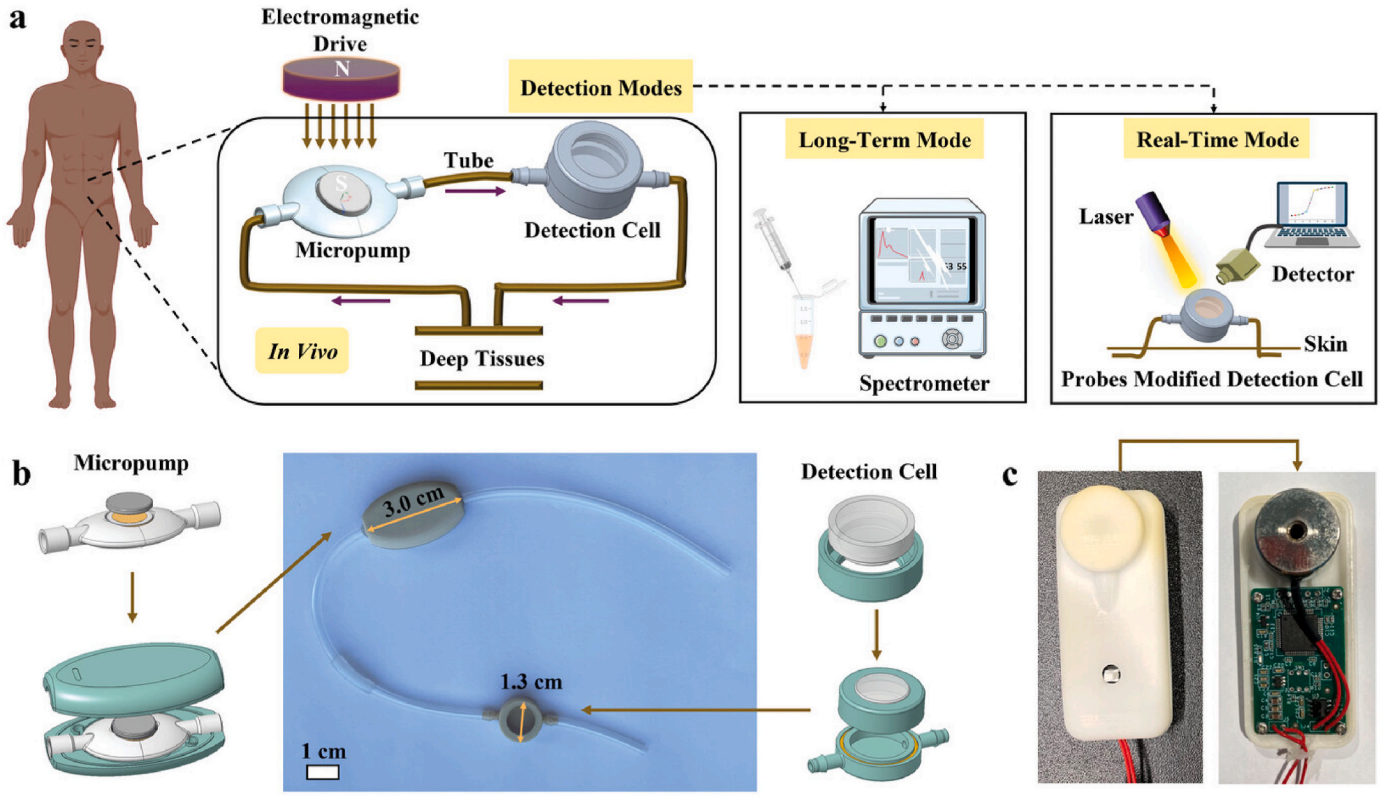

Fig. 7. Detection modes and devices using UCNP-luminescence as developed by Wang et al. a) Scheme of the developed detection modes for H_2O_2 via implantable devices. b) Structural schemes and photographs of the fabricated micropump and detection cell. c) Photographs of the electromagnetic-driven device before and after dismantling of the shell. Reprinted from Ref. [75] with permission. © 2023 Wiley.

smartphone. Based on the evaluation of the image with a network model, the differentiation between different oxidizing agents, such as permanganate, dichromate, and TATP was possible. In cuvette-based experiments and the ratiometric emission 572/447 nm of the MOFs allowed for an LOD of 2.06 nmol·L^{-1}.

2.1.3. *Non-catalytic sensing of H_2O_2*

Non-catalytic detection approaches of H_2O_2 are leaner and are often more straightforward than those requiring an additional, catalytic assay component. Typical and recent examples for the detection of H_2O_2 are probes with a boronic-ester group as a recognition element, (quenching of) aggregation-induced emission, sonochemiluminescence, and fluorescence quenching. Obviously, the lack of an enzyme or catalyst as recognition element leads to reduced selectivity as unwanted (faster) reactions with other (oxidizing) reagents occur, such as boronic-ester groups reacting non-specifically also with peroxynitrite, hypochlorous acid and peroxymonophosphate [36]. Also, the lack of a catalyst and hence increased activation energy barrier suggests that additional energy input is needed, or increased assay times occur, possibly limiting the practical application of such devices. That is the case for Dutta and Maitra's [77] paper-based approach utilizing a cholate hydrogel with the deboronation of a sensitizer ligand to then allow the energy transfer of UV-excitation light to the lanthanides Eu^{3+} or Tb^{3+}, respectively (Fig. 9). With an incubation time of 1 h and a required temperature of 50 °C the method is both time-consuming and requires an additional heating element to work. Surprisingly, the method shows reasonably good reproducibility and disc to disc variation despite the 'simple' drop coating preparation.

Cheng et al. [78] used a naphtalimide-based dye with a hexyl backbone and an aryl boronic ester moiety (C6NIB) on an aluminum foil-based silica gel plate sensing platform for the detection of H_2O_2 in vapor. They were able to detect H_2O_2 down to an LOD of 2 ppb with a detection time of only 70 s. For higher concentrations such as 30 % H_2O_2, a detection/response time of 0.5 s could be achieved. However, presumably due to difficulties regarding reproducibility in the production of the films and the and the construction-related measuring time, the authors did not carry out multiple determinations. Similarly, the group of Zhang [79] used pyrene/fluorene-based probes DB-WCZ (with two carbazole groups) forming porous microstructures enhancing the diffusion of H_2O_2 in vapor and DB-W with two aryl boronic-ester moieties, one on the pyrene and the fluorene moiety each, for the fluorometric detection of H_2O_2 and triacetone peroxide (TATP) in vapor. The spin-coated films could detect 2.2 ppb of H_2O_2 with a reasonably good reproducibility.

Xu et al. [80] integrated a fluorescent ratiometric probe for smartphone-based detection of H_2O_2 into a paper-based device or ~~into~~ a miniaturized portable 3D printed testing system with an integrated UV light excitation source. They used a flavonoid dye with an organoboron H_2O_2-reactive moiety that can bind or coordinate to the hydrophobic drug reception sites in albumin in a 1:1 ratio resulting in both, an enhancement and a blue shift of the observed fluorescence reaching an emission maximum after about 5 min assay time. In a titration assay, the flavonoid/albumin probe (HFPQ@ALB) could reach an LOD of approximately 3.5 μmol·L^{-1} and a linear range of up to 50 μmol·L^{-1}. With the smartphone application Color Desk a good linear relationship up to 200 μmol·L^{-1} H_2O_2 was achieved (Fig. 10). Here, the general disadvantages of the non-catalytic approach are overcome through the favorable hydrophobic environment in the albumin. As is true for most reactions in organic chemistry, the oxidative cleavage of boronic ester moieties and their kinetic is strongly influenced by electronic and steric coordination effects. These result in the stabilization of transition states due to solvent cages and other groups from the boronated molecule. These factors could explain some of the variations seen in the required reaction times and temperatures of the aforementioned probes and

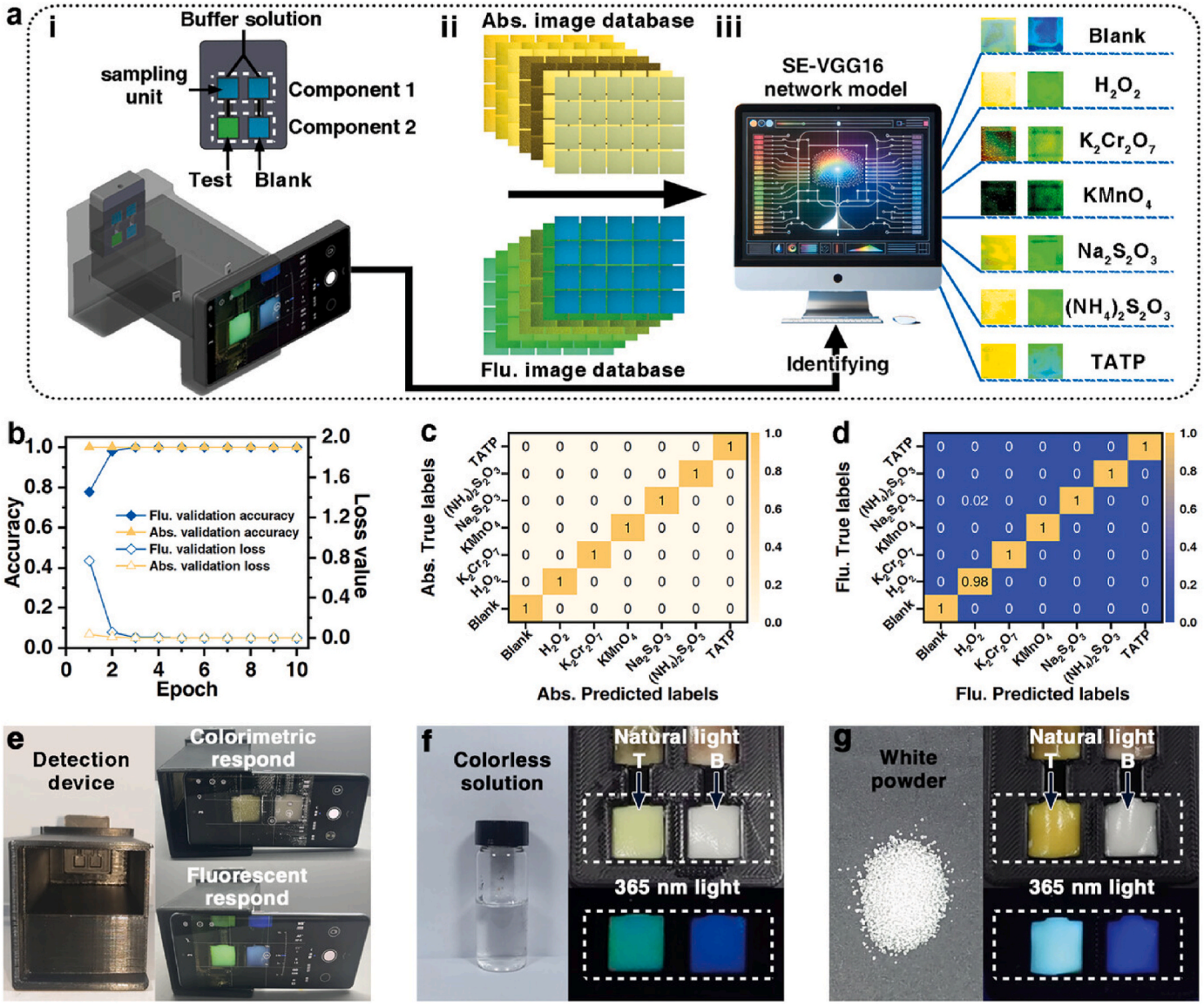

Fig. 8. Portable dual detection sensing chip by Wu et al. a) Schematic representation of the sensing chip design and image-based network model analysis. B) validation accuracy and loss values of the fluorescent and colorimetric detection modes. Confusion matrices of the c) colorimetric and d) fluorescent detection with different analytes. e) image of the 3D-printed chip/smartphone holder and colorimetric and fluorescent response on screen. f) response to colorless analyte solution with 0.3 w% H_2O_2 and g) white powder with 5 w% TATP. Reprinted with permission from Ref. [76] © 2024 Wiley.

assays.

Chang et al. [81] published a strategy for the detection of H_2O_2 and glucose on a paper-based system using an AIE fluorogen-based sensing. The proposed AIE fluorogen-based sensing strategy shows high sensitivity for H_2O_2 detection in both, solution state and on a paper-based fluorescence sensor. The paper-based assay has an LOD of 2.5 $\mu mol \cdot L^{-1}$ and a range up to 5 $mmol \cdot L^{-1}$ for H_2O_2 and 50 $nmol \cdot L^{-1}$ for glucose. An obvious disadvantage is the incubation time of 30 min at 37 °C and, if human serum is applied, the need to dilute the sample 1:10 to avoid a reduction of the fluorescence intensity (Fig. 11).

The paper-based device of Mei et al. [82] detects H_2O_2 via the quenching of the aggregation-induced emission (AIE) of Cu nanoclusters with Ce^{3+}. The detection of H_2O_2 is possible with an LOD of 3 $\mu mol \cdot L^{-1}$ and a linear range of 14–140 $\mu mol \cdot L^{-1}$. Combined with GOx, the device could be used for the detection of glucose in human serum with an LOD of 2.4 $\mu mol \cdot L^{-1}$ and a linear range of 8–48 $\mu mol \cdot L^{-1}$ showing high sensitivity and selectivity for glucose detection. The authors also claimed that glucose concentrations from 16 to 3200 $\mu mol \cdot L^{-1}$ could be discerned by eye-vision based on the color change under a 365 nm UV lamp, making rapid clinical or POC diagnostics possible. However, with a total incubation/reaction time of 40 min, the term 'rapid' diagnostics is questionable especially compared with commercially available electrochemical glucose sensors, that can provide data from whole blood within seconds.

Providing an apparative improvement the sonochemiluminescence (SCL) approach of Meng et al. [83] features an apertureless ultrasonic spray-based photoacoustic sensing platform for the detection of H_2O_2, glucose, and GOx activity. The apertureless USB-piezoelectric ultrasonic transducer (USB-PUT) overcomes the limitations of the previously established mesh-type USB-PUT, such as solution leakage and atomization, and enhances the sensitivity and intensity of the detection.

Sharma et al. [84] modified the surface of a paper-based device with a silver nanoparticle alginate composite (AgNPs@alg) for the smartphone-based colorimetric detection of H_2O_2 in a custom-made 3D printed photobox suitable for multiple smartphone models and form factors. With only 5 s of assay time (dipping into solution), detection is simple and fast, but with an LOD of 0.1 $mmol \cdot L^{-1}$ not the most sensitive approach.

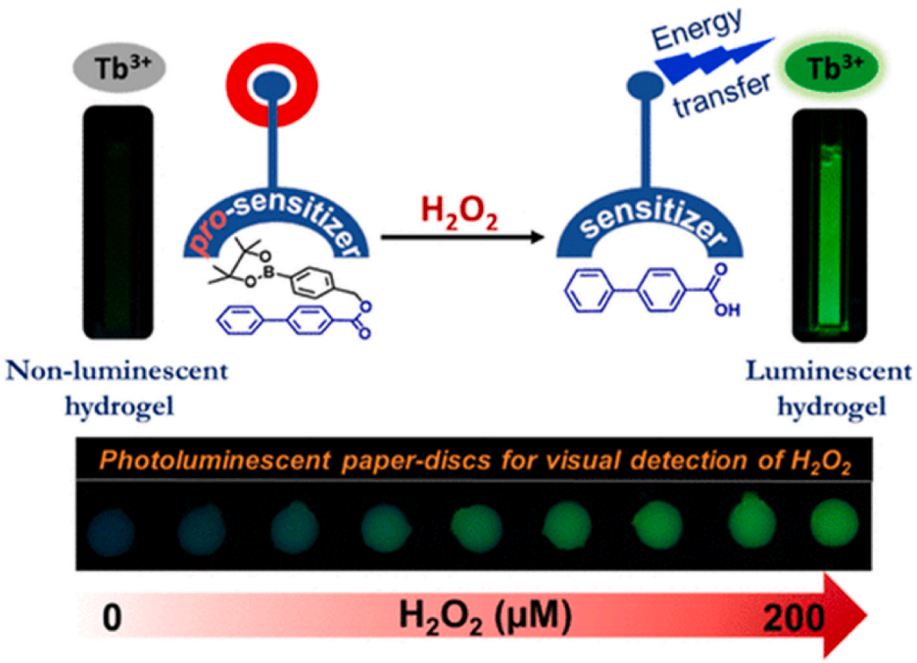

Fig. 9. Schematic representation of the sensitization of the Tb^{3+} lanthanide hydrogel and images of photoluminescent paper discs with different concentrations of H_2O_2. Reprinted with permission from Ref. [77]. ©2022 American Chemical Society.

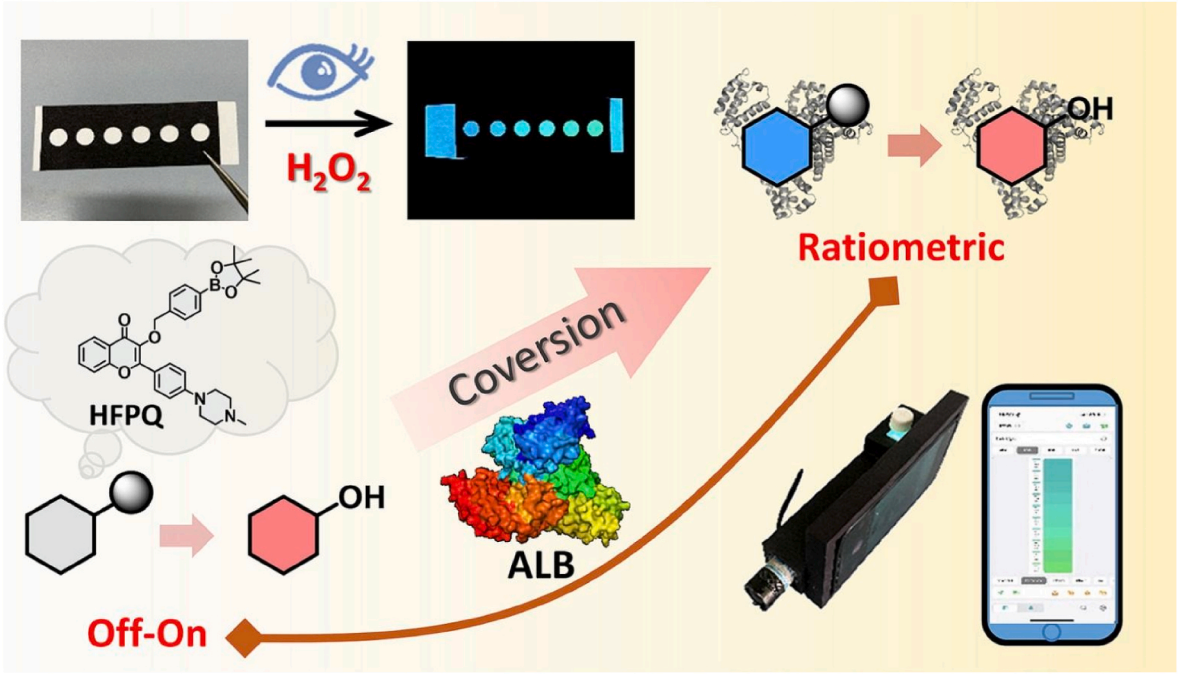

Fig. 10. Xu et al. [80] present the integration of an advanced flavonoid dye with a boronate group as recognition element embedded in albumin in a paper-based device or cuvette-based assay for smartphone readout. Reprinted with permission from Ref. [80]. ©2023 Elsevier.

He et al. [85] developed a paper-based fluorescent device for the rapid early screening of oral squamous cell carcinoma by detecting lactate and choline via the generation of H_2O_2 by GOx and LOx. H_2O_2 was detected by the fluorescence decrease of porphin-grafted composite fluorescent polymer colloids (PF-PDMTP/HQ) (Fig. 12). The signal could be detected by a grayscale value analysis of a smartphone image of the paper-based device allowing for the quantification of H_2O_2 with an LOD of 9.4 μmol·L^{-1} and a range up to 200 μmol·L^{-1}. The linear detection ranges of the grayscale value were 10–200 μmol·L^{-1} for lactic acid and 10–100 μmol·L^{-1} for choline, with LODs of 5.7 μmol·L^{-1} and 8.9 μmol·L^{-1} respectively. With the need for an UV-lamp for detection the device is not the most convenient, but with a very short assay time of only 5 min and the smartphone-based readout the method offers an intriguing and powerful opportunity for POC-care.

Unfortunately, with a few positive exceptions, many publications of single-use devices do not examine important analytical measurement parameters such as the reproducibility of the production process or the precision and accuracy of the results. Layer thickness variation for (thin)

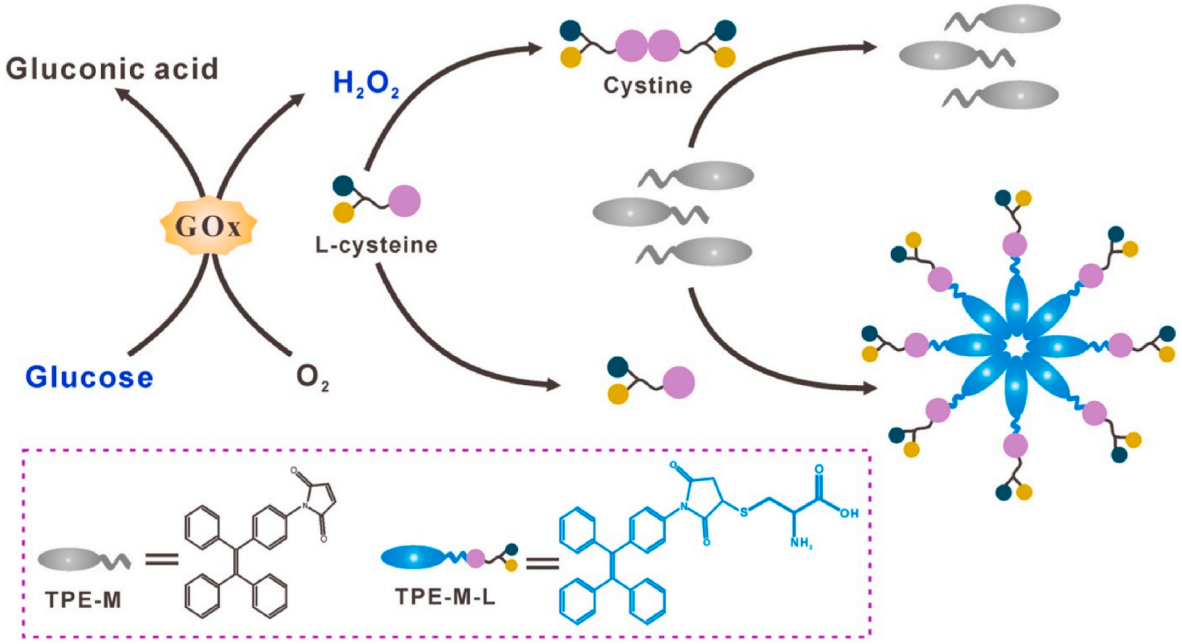

Fig. 11. Schematic illustration of the principle for H_2O_2 and glucose detection based on AIEgens. Reprinted with permission from Ref. [81]. ©2018 Elsevier.

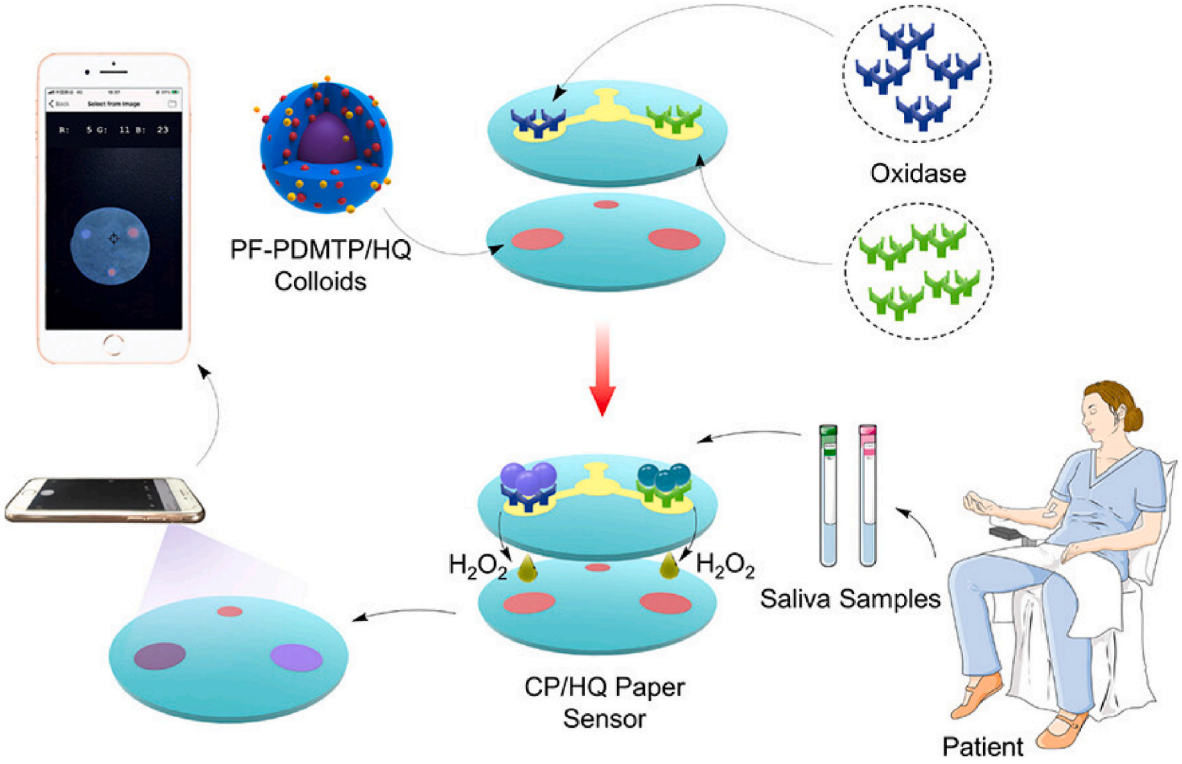

Fig. 12. Design and detection methods of CP/HQ paper-based device as presented by He et al. Reprinted with permission from Ref. [85]. ©2023 ACS.

films, coated and printed devices [86], the coffee-ring effect [87] or dispensing volume variations for drop coated and similar applications or variations from the probe carrier material or catalyst can negatively affect performance, to name a few. Unfortunately, such considerations and measurements receive too little attention although they are direly needed to evaluate the production process and all measurements. Yet, since manual preparation in the lab cannot provide the precision provided by mass-produced devices, and since additional significant effort is needed to produce such results, too many academic scientists shy away from presenting such potentially difficult data.

2.2. *The complexity of smartphone-based optical data acquisition*

With several groups using smartphones in previously mentioned publications, one cannot and should not avoid addressing the issue here. The dramatic improvement of camera and imaging technology of smartphones enables researchers to use them for data recording of sensor signals [88–90] and in general as transducers and photon

detectors for optical applications. Smartphones can represent a compact and user-friendly detection system for performing various chemical assays, enabling real-time, on-site, and point-of-care testing. This shift from traditional laboratory-based analyses to portable, smartphone-integrated approaches broadens the accessibility of chemical testing away from the lab toward the general public. In contrast to photoluminescence, chemiluminescent [56,71] and colorimetric applications [25,40,63,91] generally require no additional external light source, making the latter two the preferred detection methods in the readout of analyte concentrations with smartphones.

The constant evolution of smartphone cameras and the variation between models brings forth a substantial challenge for standardization and hence universal applicability in analytical systems. While the ongoing advancements enable more sensitive and sophisticated detection methods, the plethora of choices in the smartphone market makes it challenging to create detection cabinets and protocols that can seamlessly integrate with every model. Each smartphone model possesses unique features, dimensions, camera specifications, positioning of the camera on the smartphone, software (availability & compatibility) and sensor configurations, leading to variations in light detection performance and potentially compromising the reliability of analytical results, a factor typically overlooked or ignored in papers featuring smartphones as detection platform. Specifically, most researchers are content to demonstrate the feasibility of their studies with one specific smartphone model and one operating system and do not provide general applicability. Moreover, the abundance and widespread availability of smartphones are often touted as major selling points and primary reasons for utilizing them in analytical applications. However, the very characteristic that makes smartphones attractive for widespread use becomes a double-edged sword. The allure of accessibility can lead to a lack of thorough consideration for the challenges posed by the diversity of smartphones.

With regard to the measurement setup or measurement design, one should ask oneself in many publications why, if a simple and portable low-effort system is to be developed for 'everyone', the complex and time-consuming calibrations should not also be simplified. Especially for colorimetric and reflectometric measurements, the addition or rather integration of a calibration color-bar or code (as is already used in a variety of indicator and test strips [92]) should do the trick. Thinking onward: With the current developments and interest in machine-learning and image analyzing AI, future applications in detection and analysis with smartphone based apps could also greatly benefit from that development with some groups already applying that to basic colorimetric systems [93].

The lack of standardized reporting of operational parameters used in smartphone-based detection in publications exacerbates this issue. Without comprehensive information on the specific parameters and settings used in experiments, the reproducibility of results becomes a daunting task. Researchers aiming to replicate or build upon these studies may face difficulties in achieving consistent outcomes without a clear understanding of the operational intricacies tied to specific smartphone models. Ideally, parameters that would be published are (if available) used aperture, shutter speed, white balance, ISO-value, color space, data format (e.g. JPEG, RAW, TIFF, etc.; with only RAW files representing real image data unbiased by the camera software), type of (CCD or CMOS)sensor, software version of image-capturing software and used automated image processing routines by the camera software (if so), and the used illumination source. Such datasets should become standard or at least be a standard to that should be striven for to warrant replicability of analytical detection with smartphones and contribute to let them become a more accepted means of detection rather than a trendy additional detection system.

The need for adaptability across different smartphones and operating systems is crucial for the advancement and acceptance of smartphone-based analytical systems. Collaborative efforts within the scientific community, involving researchers, developers, and industry stakeholders, are essential to establish guidelines for reporting operational parameters and creating adaptable detection cabinets. Such guidelines would ensure a more systematic approach to smartphone-based analytical research, fostering standardization and improving the overall robustness and reliability of these systems. This issue is gaining attention, with different groups on the scientific side proposing such standards for reproducible reporting and data acquisition [94,95], open source software for image analysis [96], digital color analysis [97], color correction algorithms [98] and positive influences arising from microscopy applications [99].

3. Sensors, intermediate and semi-reversible sensing systems for quantitation of H_2O_2

Many applications including environmental analysis, process, biomedical and general cell culture monitoring, will greatly benefit from a constant monitoring of H_2O_2 or precursor analytes [100]. Overall, development of such continuous and fully reversible optical sensors has been slow since their tasks are significantly more challenging. The well-known interferences and problems such as (bio)fouling [101], photobleaching, general changes in the composition of the analyte matrix including variations in pH, ionic strength, leakage of probe molecules and temperature are all dramatically enhanced challenges for continuous sensors. Intermediate and semi-reversible strategies can in some instances provide a sufficient solution through the help of an appropriate engineering and assay design.

3.1. *Intermediate and semi-reversible sensing systems for quantitation of H_2O_2*

Intermediate and semi-reversible systems represent the stepping-stone between discontinuous single-use sensors and continuous fully reversible sensors. These systems allow semi-continuous detection by repeated sample injection with irreversible reactions, with steadily or repeated input of reagents, such as flow injection analysis (FIA) or external factors such as light, temperature, addition of redox reagents or cycling by an applied potential to allow (sufficiently fast) regeneration of the sensing capability.

3.1.1. *FIA systems*

Due to the in-flow addition of buffer and reagents, FIA systems can work with a variety of sample types and concentration ranges with a broad range of pH values, assuming a sufficient dilution and buffering can be reached. The noteworthy recently developed FIA-protocols are mostly CL-based. Aside from the advantage of not requiring an excitation lamp, thus reducing the required number of optical components, CL reactions often show rapid to seemingly instantaneous kinetics, the temporal resolution therefore being mostly defined by instrumental limitations. However, requiring a certain level of instrumentation with pumps, waste disposal, reagents, buffers and the like combined with a temperature dependence of CL reactions, such FIA systems are not the preferred choice for remote or POC applications. As the injected samples are being 'contaminated' with reagents and buffers such systems are also not applicable to 'closed loop' systems and are not ideal for very small sample volumes.

Advances both in instrumental nature and on the basis of reagent additives were key to the work by Moβhammer et al. [102] (Table 2) who developed a versatile FIA system coupled with microdialysis probes allowing an initial size exclusion to avoid contamination of the system with larger molecules for the sensitive detection of H_2O_2 with an acridinium ester as CL reagent (Fig. 13). Their protocol and setup offers customizable calibration ranges and exhibits enhanced selectivity, especially with the addition of EDTA to prevent commonly occurring interference from metal ions such as Fe(II) and Fe(III) [103].

As with single-use devices, also enzyme mimics are seeing their use in FIA systems. For example Li et al. developed a [104] CL FIA protocol

Table 2
Intermediate and semi-reversible sensors for the detection of H_2O_2 presented in this review.

Probe/recognition element	Detected signal	(LOD) Analytical/calibration Range(s) of H_2O_2	conditions	Regeneration condition/cycle time & condition	Ref
acridinium ester	CL	0–1000 nmol·L^{-1}; 0–10 µmol··L^{-1}; 1–100 µmol··L^{-1}		FIA	[102, 103]
Luminol/Fe-PorCOF	CL	(5.3 nmol·L^{-1}) 0.01–10.0 µmol·L^{-1}	carbonate buffer pH 10.5	FIA	[104]
SPAN/HKUST-1@Luminol	CL	(60 nmol·L^{-1}) 0.1–30 µmol·L^{-1} (25 pmol·L^{-1}) 30–600 pmol·L^{-1}	pH 7.4 PBS 0.1 mol•L^{-1} NaOH.	FIA	[105]
TCPO/Carbon nanodots	CL	(11.7 µmol·L^{-1}) up to 15 mmol·L^{-1} (linear); up to 50 mmol·L^{-1} (exponential fit)		FIA	[106]
WS_2 QD NaCLO	CRET	(38 nmol·L^{-1}) 0.14–14 µmol·L^{-1}.		FIA	[107]
Amplex Red/HRP	HRP/H_2O_2 oxidation of Amplex Red to resorufin	(0.05 µmol·L^{-1}) 0–49 µmol·L^{-1}	1/6 dilution with buffer	FIA, washing with buffer 15 min	[108]
CeO_{2-x} NPs	Luminescence quenching	n.a.		36 min UV light +52 °C	[110]
CoHCF	Absorbance	1.5–20 mmol·L^{-1}		Redox Cycle	[111]

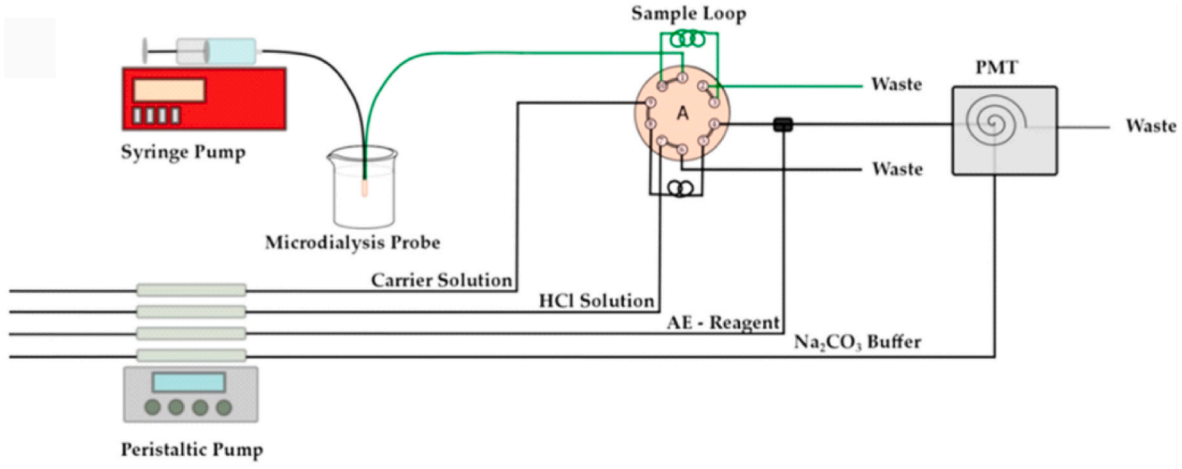

Fig. 13. Schematic of the FIA setup developed by Moβhammer et al. with microdialysis probe for sample uptake with a syringe pump. The reagent and buffer additions are achieved with a with peristaltic pump. Reprinted from with permission [102]. ©2018 Elsevier.

using a Fe-porphyrin covalent organic framework (Fe-PorCOF) as peroxidase mimic combined with luminol for H_2O_2 detection and a broad linear range of 0.01–10.0 µmol·L^{-1} and an LOD of 5.3 nmol·L^{-1} in carbonate buffer pH 10.5. Aside from the use of the enzyme mimic, the FIA protocol and setup were standard.

Yuan et al. [105] realized a CL FIA approach through a sulfonated polyaniline decorated copper-based metal organic frame composite (SPAN/HKUST-1@Luminol). This composite has a significantly enhanced CL quantum yield of 136 times higher than luminol and showed good signal intensities not only in basic conditions, but also at physiological pH of 7.4. In a PBS pH 7.4 running buffer, they were able to detect H_2O_2 with an LOD of 60 nmol·L^{-1} with a linear range of 0.1–30 µmol·L^{-1} and in 0.1 mol·L^{-1} NaOH down to 25 pmol·L^{-1} with a linear range of 30–600 pmol·L^{-1} (Fig. 14). Thus, combining their system with an autosampling setup would make a very interesting setup for monitoring H_2O_2 in cell cultures. In another study, Shen et al. [106] published a FIA protocol integrating carbon nanodots (CDs) and bis(2,4,6-trichlorophenyl) oxalate (TCPO) for sensitive quantification of H_2O_2 and glucose with an LOD of 11.7 µmol·L^{-1} and a wide linear range up to 15 mmol·L^{-1} with the option for an exponential fit extending the quantitation range up to 50 mmol·L^{-1}. Most notably, the CL quantum yield of the CDs reached $(8.22 \pm 0.30)\cdot10^{-3}$ which the authors claim is among the best values reported for a CL nanomaterial used in chemical analysis. New in their system is the use of these enhanced CL-carbon dots, whereas the FIA protocol itself is a traditional strategy.

In the case of Sun et al. [107] a chemiluminescence resonance energy transfer (CRET) platform is proposed that utilizes WS_2 quantum Dots (QDs) for assessing H_2O_2 during photocatalytic processes, achieving a low LOD of 38 nmol·L^{-1} and a linear range from 0.14 to 14 µmol·L^{-1}. This is especially interesting for future applications on the analysis and evaluation of disinfectant properties of photocatalytic species.

A unique strategy to overcome problems with both the autofluorescence/color of erythrocytes and the time-factor of measuring H_2O_2 from whole blood samples is proposed by Sen et al. [108]. By using an acoustics-based blood plasma separation module in their microfluidic setup, they were able to remove interfering and H_2O_2-degrading contents and quantify H_2O_2 from fresh whole blood samples in one setup in flow. The separated plasma was then mixed in the microfluidic chip with HRP, buffer and Amplex Red which could be measured on-chip and off-chip in their setup. In the on-chip separated plasma the group was able to detect H_2O_2 in a range of 0–49 µmol·L^{-1} and with an LOD of 0.05 µmol·L^{-1} within a total response time of 15 min. For healthy individuals the group reported H_2O_2 values in the range of 0.8–6 µmol·L^{-1} in whole blood. While microfluidic systems do allow a miniaturization of the actual mixing and measurement modules, and in this case also makes centrifugation obsolete the previously mentioned same restrictions as for the other FIA systems apply, but by using a microfluidic system, they were able to reduce the required sample, buffer and reagent volume in comparison with a larger FIA setup. By choosing a photoluminescent reagent, the setup naturally also requires an excitation light source or laser, respectively. The results suggest that the setup could be applied also to rapid blood screening (Fig. 15).

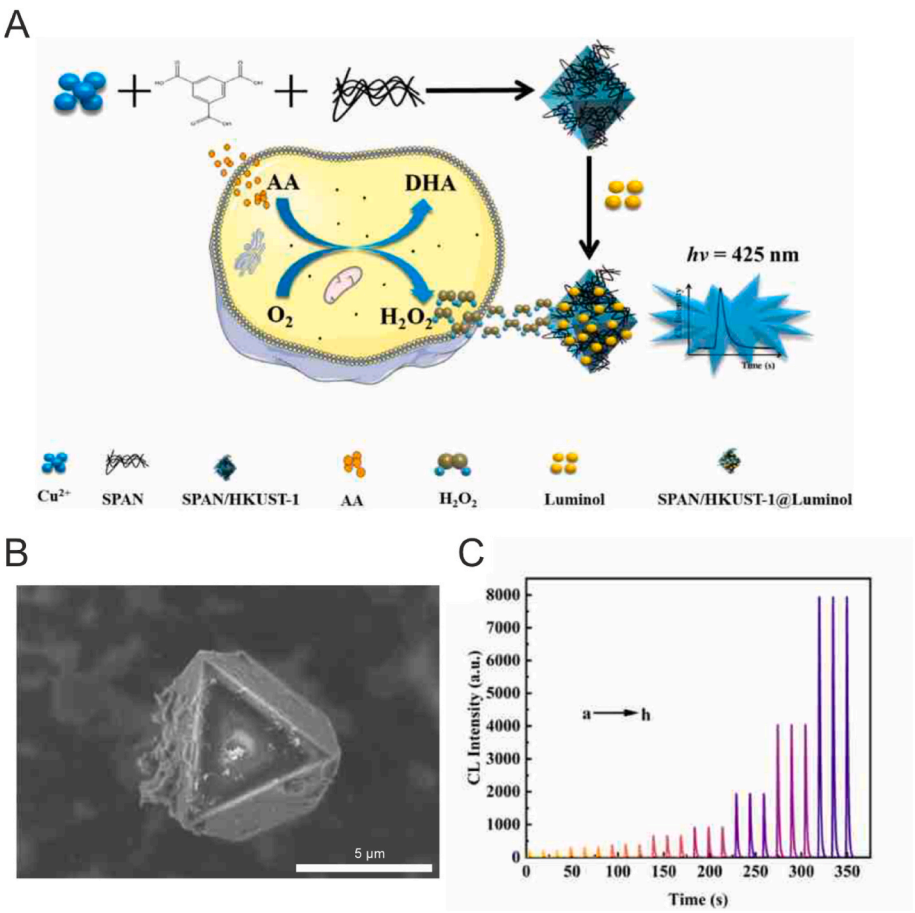

Fig. 14. **A** Schematic diagram of synthesis of SPAN/HKUST-1@Luminol composite and the mechanism of the CL detection of H_2O_2. **B** SEM image of SPAN/HKUST-1@Luminol **C** CL responses of the SPAN/HKUST-1@Luminol in PBS (pH 7.4) toward different concentrations of H_2O_2 (from a to h, 0.1, 0.7, 1, 2, 3, 7, 15, 30 μmol·L^{-1}). Reprinted with permission from Ref. [105]. © 2023 Elsevier.

3.1.2. *Regeneration of the detection system by external factors*

Reversibility of a detection strategy was proposed by Malyukin et al. using CeO_{2-x} NPs [109]. These NPs can detect H_2O_2 by oxidation of Ce^{3+} to Ce^{4+}. This is accompanied by quenching of Ce^{3+} luminescence of the nanoceria at 430 nm by a Fenton-type reaction as the nanoceria particles also show a peroxidase-like activity. However, the long regeneration time of the nanoparticles of up to 120 h at 22 °C or 24 h at 37 °C for the smaller, 2 nm nanoparticle species, with the larger 10 nm nanocrystals taking even longer for their regeneration required faster conversion to make this approach competitive to other methods. Later, Seminko et al. [110] discovered, that by simultaneously increasing the temperature and continuous irradiation with UV light, they were able to reduce the regeneration time for the H_2O_2 detection of CeO_{2-x} and CeO_{2-x}:Eu^{3+} NPs from 180 h to 4 h down to 36 min at 52 °C respectively. These reduced regeneration times might not be sufficient for applications that require constant monitoring but could be suitable for applications where a high temporal resolution is not required. In combination with a currently severely limited capability of quantitation this technology requires further development and improvement before being implemented into a functional sensing device.

Cobalt(II)-hexacyanoferrate (CoHCF) was used as an advanced Prussian white substitute by Virbickas et al. [111] as an optical indicator for H_2O_2 which is electrochemically regeneratable as a layer on an ITO/glass substrate. This unique system shows high stability of CoHCF's thermochromic properties after voltammetric cycling and also resistance to air exposure. The needed constant temperature of 25 °C for photometric detection seems to be a minor disadvantage that can be overcome with a simple chip-controlled temperature module (Fig. 16).

3.2. *Continuous and fully reversible sensors for quantitation of H_2O_2*

The interplay between signal response, recovery, interferences, calibration, and long-term signal drift distinguishes continuous and fully reversible sensors from discontinuous or single-use sensors. In the case of H_2O_2 detection, sensors should show rapid response times, allowing for real-time detection of concentration changes in a dynamic environment as this timely information enhances safety, efficiency, and overall process optimization. For all new concepts proposed, it is hence very important to understand the mechanisms underlying the reversibility as only this will allow smart optimization of the sensor performance ensuring their longevity in demanding applications.

Publications over the last five years have proposed valuable new concepts and probes for continuous and reversible optical sensors for H_2O_2. Such concepts address photobleaching, leakage, internal referencing, reduction of interferences and background signals.

3.2.1. *Ratiometric fluorescence*

Dung and Rhee [112] (Table 3) immobilized HRP on the surface of a sol-gel glycidoxypropyl trimethoxysilane and aminopropyl trimethoxysilane membrane containing carboxyl group functionalized-CdSe/ZnS quantum dots (QDs) and aminofluorescein (AF)-encapsulated polymer particles as probe and reference material, respectively. The membranes were excited at 400 nm and measured at 500 nm for the reference and at 560 nm for the QDs, respectively. In presence of H_2O_2, the luminescence of the QDs was quenched allowing a detection of H_2O_2 with a calculated LOD of 11 μmol·L^{-1} and a linear range of 0.1–1 mmol·L^{-1} with a response time of 5.5–8.5 min. The membrane also showed an acceptable

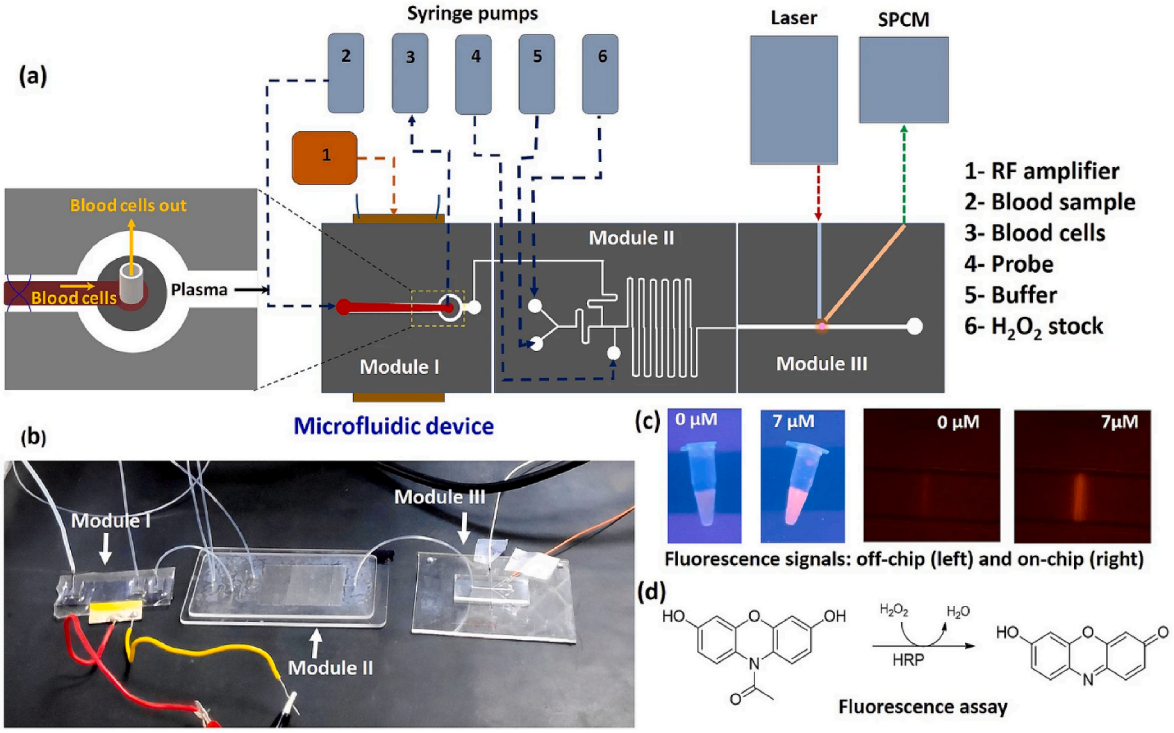

Fig. 15. Sen et al. developed a microfluidic FIA-device for the detection of H_2O_2 in whole blood with a blood separation device on-chip. (**a**) Schematic of the microfluidic device with blood separation (module I) reagent and buffer addition and mixing (module II) and detection (module III) (**b**) photograph of the microfluidic device and the respective modules, (**c**) images of the fluorescence in a reaction cup and in the channel (**d**) Amplex Red reaction with H_2O_2 in presence of HRP. Reprinted with permission from Ref. [108]. © 2021 Springer. (For interpretation of the references to colour in this figure legend, the reader is referred to the Web version of this article.)

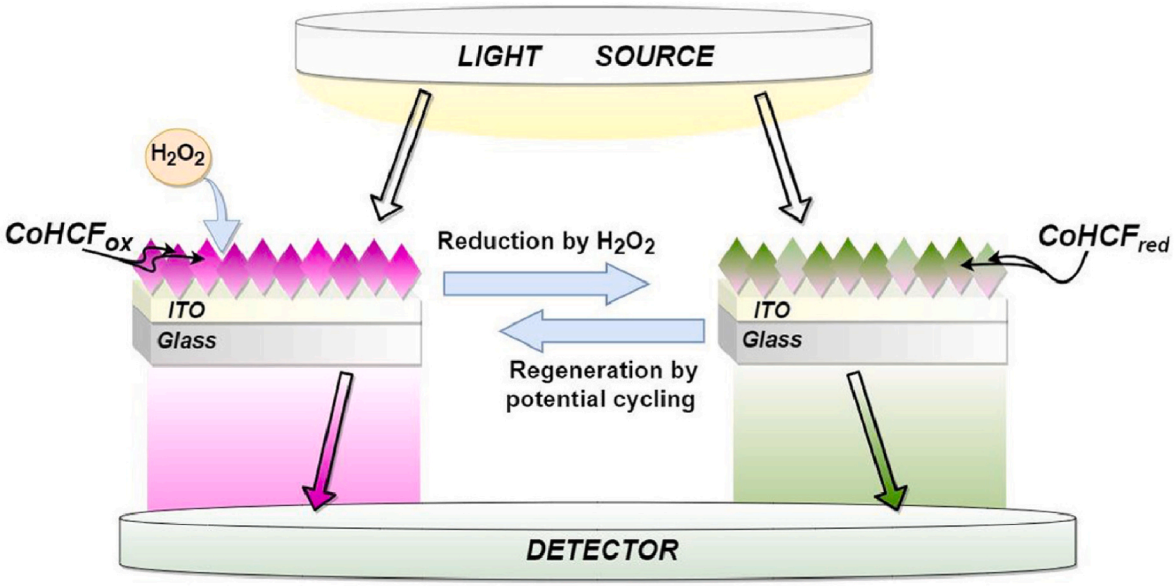

Fig. 16. Scheme of the semi-reversible Cobalt(II)-hexacyanoferrate (CoHCF) sensor as published by Virbickas et al. Reprinted with permission from Ref. [111]. ©2020 Elsevier.

reusability and stability of the signal after 60 test runs for concentrations up to 1 mmol·L^{-1} whereas for higher concentrations (up to 10 mmol·L^{-1}) the response of the membranes was reduced. The authors attribute this reduction in sensitivity to the polymer backbone degradation. By using QDs, the sensor eliminates the issue of photobleaching if one ignores the photobleaching of the reference (AF)-encapsulated polymer particles. On the negative side, QDs innately also show a blinking emission, an issue usually easily remedied by longer integration time of the signal. With the rather long response time and a limited useable analytical range further research in the field is required (Fig. 17).

3.2.2. SPR-based detection

The label-free SPR technique has long been used in flow-systems

Table 3
Reversible sensors for the detection of H_2O_2 presented in this review.

Probe/recognition element	Detected signal	Sensor type	(LOD) Analytical Range of H_2O_2	Conditions	Response time	Ref
Carboxyl group functionalized-CdSe/ZnS	Ratiometric fluorescence/fluorescence quenching	GPTMS/APTMS hydrogel membrane	(11 μmol·L^{-1}) 0.1–1 mmol·L^{-1}			[112]
GO nanosheets/catalase	SPR curve shift	SPR Flow Cell	(55 μmol·L^{-1}) up to 1000 μmol·L^{-1}		30 s	[114]
PtTFPP in D4 membrane KCC-1-PEI/PtNPs in D4 membrane	Oxygen quenching of PTFPP emission by catalase-like mimic degradation of H_2O_2	Hydrogel membrane based	(15 μmol·L^{-1}) 1 μmol·L^{-1} - 10 mmol·L^{-1}		<1 min for 3 mmol·L^{-1} H_2O_2 up to 6 min for other concentrations	[117]
PtTPTBPF/PdTPTBPF	RuO_2/PtNP catalyzed degradation of H_2O_2 with O_2-quenching of PtTPTBPF and PdTPTBPF phosphorescence	Flow-cell based	(0.17 μmol·L^{-1}) (0.16 μmol·L^{-1}) Up to 1000 μmol·L^{-1}	PtNP spots RuO_2 spots	4.6 min total, ≈2.5 min retention time 5 min equilibration	[118]

making it applicable for in-situ measurements. It enables very fast response times and depending on the setup it may only require small sample volumes. As label-free strategy that monitors activity at the sensor surface, it obviously suffers from non-specific interactions and adsorption processes [113]. Gupta and Semwal [114] proposed an enzymatic decomposition of H_2O_2 to O_2 and H_2O, where the latter interacts with graphene oxide (GO) nanosheets in the GO/gold wafer interface. This interaction causes a change in the refractive index and a shift in the resonance wavelength of the SPR curve. Unfortunately, the authors opted for discontinuous FIA-style operation and did not take advantage of an in principle possible continuous measurement set-up. Nonetheless, the sensor showed a response time of 30 s, an LOD of 55 μmol·L^{-1} and a quantitation range up to 1000 μmol·L^{-1} (Fig. 18).

3.2.3. Oxygen-based H_2O_2 detection

The well-known and well-published concept of quantifying H_2O_2 through catalytically or enzymatically generated oxygen followed by quenching of fluorescence or phosphorescence [115] allows the use of several well-established oxygen-sensitive dyes and complexes as probes, such as Ru-bipyridines, Ru-Phenanthrolines and Pt- and Pd-porphyrins [116]. Major advantages of this approach include probe response time and regeneration time with the quenching mechanism being primarily diffusion limited. Obviously, residual oxygen or oxygen concentration changes within the samples can severely impact measurement quality, reproducibility, and precision and must be taken into consideration. Ding et al. [117] present a sensor employing Pt NPs within fibrous silica particles embedded in a hydrogel matrix, demonstrating promising detection capabilities and requiring only very small sample volumes. Unfortunately, they noticed a luminescence decrease of 12 % after the first calibration cycle, which they attributed to leakage. Aside from that, they also observed concentration-dependent response times and, while acknowledging the issue of interference from residual oxygen and temperature in principle only briefly suggested possible solutions, i.e. the integration of oxygen and temperature control sensing spots. The work of Torsten Mayr's group [118] which they were recently also able to use as detection element for at-line monitoring of H_2O_2 released from a photocatalytic synthesis [119] offers an innovative flow-cell-based sensor with an additional oxygen sensing element and an upstream deoxygenation module to mitigate such baseline issues and sensory drifts based on oxygen changes as in their previously published glucose sensor (Fig. 19) [120]. While achieving enhanced LODs, extended linear ranges, full reversibility, stable hysteresis, and stability over 9 h of measurement, the sensor's response/equilibration time of 5 min, the batch-to-batch variation and complexity associated with the experimental setup underscore the need for further refinement and consideration of practical application challenges.

4. Conclusion and outlook

The development of optical H_2O_2 sensors shows a clear trend toward implementing synthetic enzyme mimics and nanozymes as tunable and efficient replacements for peroxidases. Although some aspects, regarding catalytic activity, issues with the vague interpretation of the definitions and wording are under scrutiny, the hope is that these nanomaterials can provide a better long-term and assay stability in addition to desirably low LOD's. Nevertheless, benchmark experiments and closer comparison to enzyme activities and nanozyme weight- or amount-based turnover rates should be included in publications for better classification. The next steps towards their possibly broad-based use in analytical systems are the comprehensive design of studies investigating their effect on the environment including toxicity, persistence, (bio)accumulation, and overall environmental impact [121]. In fact, some of the heavy metal-based systems may be far from any sustainable use. It is therefore of great interest that some efforts are made searching for renewable sources of educts for the synthesis of certain enzyme mimics [122–124].

For colorimetric applications, TMB continues to be the most common indicator, despite the availability of other valid options such as Amplex Red, nanomaterials or ABTS. This increased use is likely due to its commercial availability, comparably low price, and an abundance of protocols for enzymes and synthetic enzyme mimics. However, finding a replacement for colorimetric substrates with a broader dynamic range, lower background signal and lower environmental impact would be highly desirable. Considering the vast number of published enzyme mimics, there may be a possibility of new developments and applications on this front in the future.

The dramatic improvement of cameras integrated in smartphones has made those an easy transducer for sensor development as signals can easily be taken and processed through appropriate apps. This clearly is a significant and growing, but not entirely unproblematic trend in the field of analytical chemistry [90]. The paradigm shift from lab-based detectors to smartphone cameras is driven by the widespread use, computational power, and portability of modern smartphones, which have transformed these handheld devices into versatile tools for quantitative chemical analysis. Smartphone-based detection is also commonly used with paper-based sensors combining low-cost and weight disposable sensors and broadly available smartphone devices. However, standardization of smartphone optical data acquisition and its software conversion to work with smartphones from any producer still remains an unsolved task. Specifically, comprehensive reporting of experimental parameters regarding image capture and data/software processing, is necessary for reproducibility and reliability in smartphone-based detection. The diversity of smartphone models does pose a challenge for standardization and universal applicability in analytical systems. Efforts to adapt measurement setups to accommodate different models and operating systems are crucial. In combination, performing control experiments with different smartphones are needed to show the robustness and versatility of sensing platforms. The implementation or integration of simplified calibration processes such as standard color bars or codes into measurement designs to facilitate

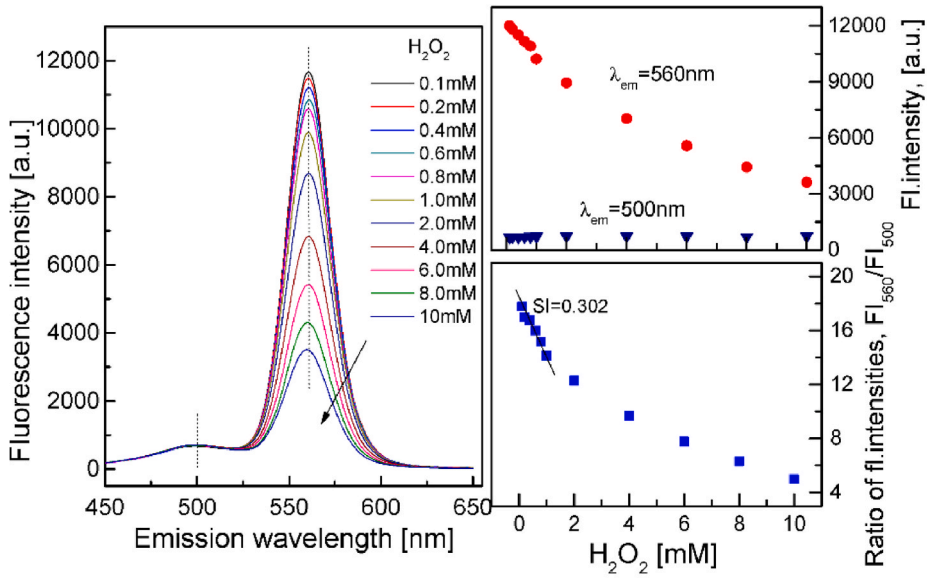

(a)

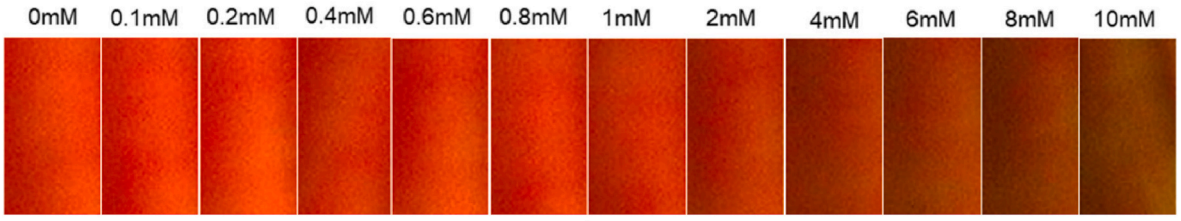

(b)

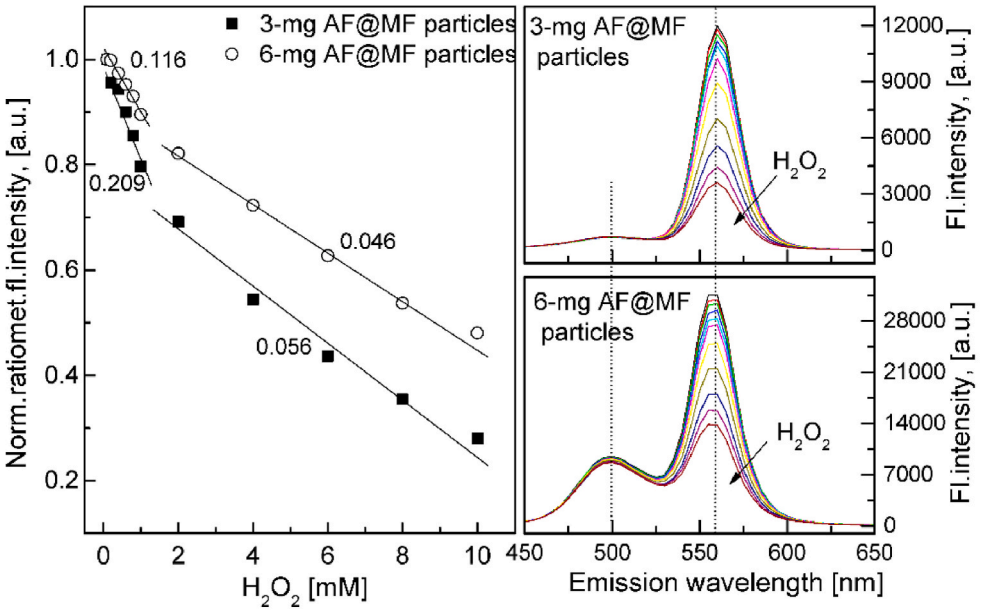

(c)

Fig. 17. (a) Emission spectra of QD–AF membrane at different concentrations of H_2O_2 and its calibration curve for H_2O_2 determined by normalization of the fluorescence intensities (FI560/FI500). (b) Images of fluorescence quenching of the QD–AF membrane after exposure to increasing H_2O_2 concentrations. (c) Calibration curves and response of the QD–AF membranes in H_2O_2 at concentration ranges of 0.1–1 mmol·L^{-1} and 1–10 mmol·L^{-1} using a small (3 mg) or large (6 mg) amount of reference dye particles. Reprinted with permission from Ref. [112]. © 2019 MDPI.

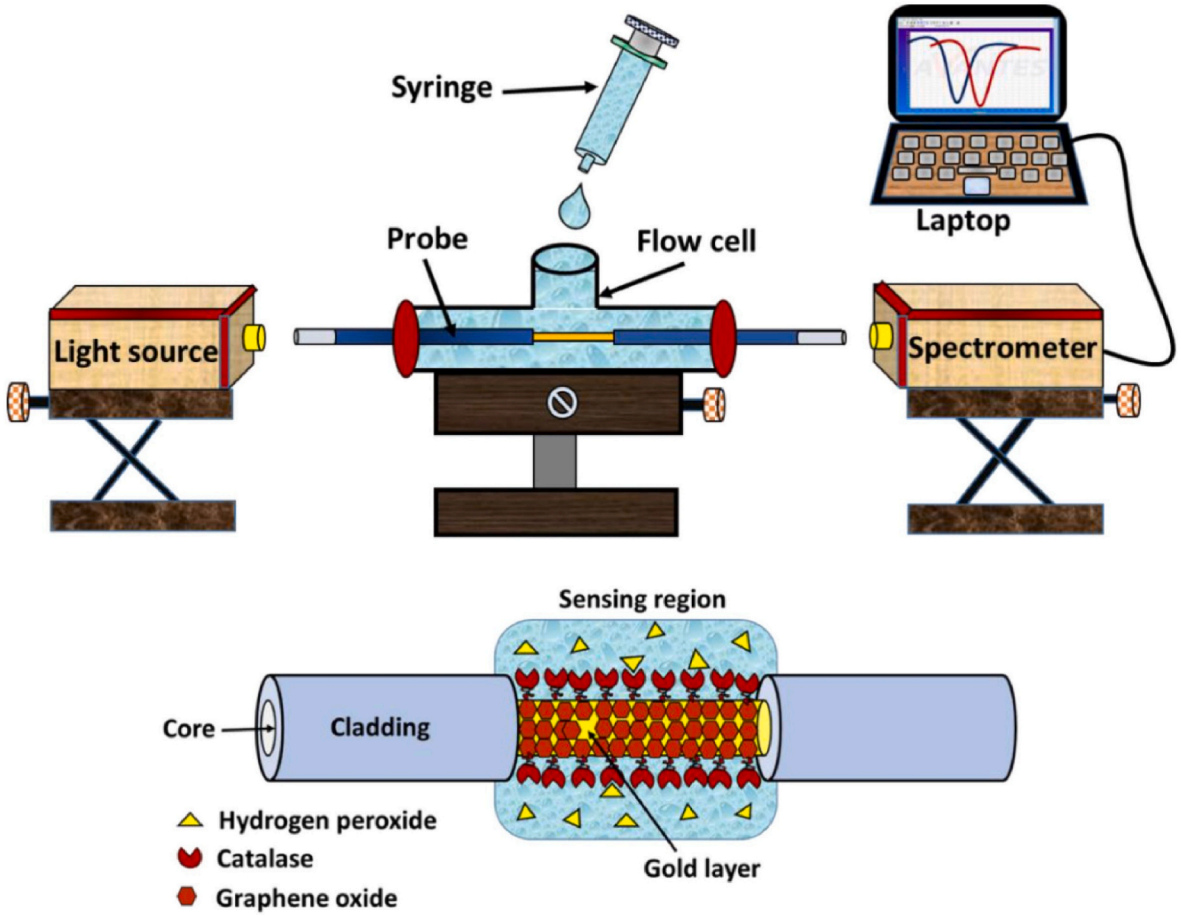

Fig. 18. Schematic diagram of SPR sensing setup and probe design as proposed by Gupta and Semwal. Reprinted with permission from Ref. [114]. © 2021 Elsevier.

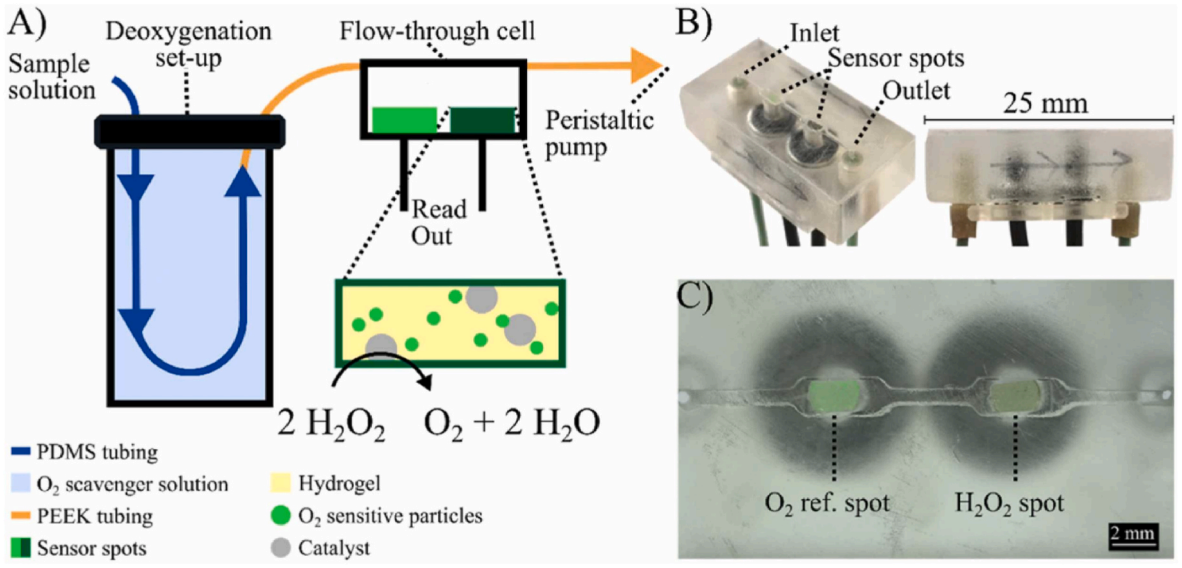

Fig. 19. A) Schematic and B) picture of the flow cell of the oxygen sensor with C) O_2-reference and H_2O_2 detection spot developed by Torsten Mayr's group. Reprinted with permission from Ref. [118]. ©2023 Elsevier.

ease-of-use for a wide range of users in different lighting and (smartphone) camera situations could also improve sensing accuracy and accessibility.

Overall, such collaborative efforts within the scientific community are needed and are being actively pursued [92,94–99] to establish guidelines for reporting operational parameters and creating adaptable detection systems. This would promote standardization and improve the reliability of smartphone-based analytical research. Such standards from researchers for researchers will help development and innovation and serve as a benchmark, as well as provide regulatory institutions with

helpful examples for developing operational guidelines and requirements.

The current rise of machine-learning algorithms and AI-tools could also provide a massive enhancement for image and data analysis for both smartphone-based mobile and more classical laboratory-based applications. This trend leans on early research in the 1990s using neural networks for pattern recognition [125]. A main hurdle will always be the sheer amount of data that is needed to feed such digital learning tools but considering current trends and openness from funding agencies to go along this developmental route, the integration of AI in sensors and sensing technology will become not only feasible but also useful.

Although an abundance of novel photoluminescent probes is developed and published, the number of sensors based on new probes is limited. Literature surveys show that over 1152 papers alone are found in the Web of Science since 2018 when searching for 'fluorescence detection hydrogen peroxide'. Yet, these are seldomly picked up by researchers developing optical sensors, who tend to use established probes. One may ask why this disconnect exists. Don't the new probes address challenges hampering optical sensors? Or do sensors lag behind probe development? Obviously, there should be more interaction between these two research fields. If there was more cooperation here, great sensors would surely come to or rather emit light (with a higher wavelength).

For the semi-reversible/continuous systems FIA methods, especially in combination with CL reagents, have seen improvement and have shown to be powerful tools. With the developments based on newer, brighter CL reagents, microfluidics, portable systems useable for more remote work [126] and the improved sampling systems, new innovations and better systems are just around the corner.

Clearly, fully reversible and continuous optical H_2O_2 sensors remain a rarity where to-date no fully satisfying solution exists. Yet, the development of probes or recognition or catalytic elements alone is not sufficient. It is also necessary to develop new, sustainable membrane coatings that protect optical probes from fouling and leaking. Self-referencing or ratiometric probes are needed to avoid extensive calibration and sensory drifts. Novel probes with a truly reversible detection mechanism that work not only in cuvettes but can be used in sensor membranes and for continuous detection are required. We thus think that this should motivate the leading minds in sensor and optical probe development to enhance collaboration towards the advancement of superior optical sensors addressing the critical issues here described that are beyond each single lab's expertise.

CRediT authorship contribution statement

John J. Galligan: Writing – original draft, Conceptualization. **Antje J. Baeumner:** Writing – review & editing, Conceptualization. **Axel Duerkop:** Writing – review & editing, Conceptualization.

Declaration of competing interest

The authors declare that they have no known competing financial interests or personal relationships that could have appeared to influence the work reported in this paper.

Data availability

Data will be made available on request.

References

[1] X. Liu, C.N. Kim, J. Yang, R. Jemmerson, X. Wang, Induction of apoptotic program in cell-free extracts: requirement for dATP and cytochrome c, Cell 86 (1996) 147–157, https://doi.org/10.1016/s0092-8674(00)80085-9.

[2] E.A. Veal, A.M. Day, B.A. Morgan, Hydrogen peroxide sensing and signaling, Mol. Cell 26 (2007) 1–14, https://doi.org/10.1016/j.molcel.2007.03.016.

[3] P.M. Vanhoutte, H. Shimokawa, M. Feletou, E.H.C. Tang, Endothelial dysfunction and vascular disease – a 30th anniversary update, Acta Physiol. 219 (2017) 22–96, https://doi.org/10.1111/apha.12646.

[4] E.W. Miller, O. Tulyathan, E.Y. Isacoff, C.J. Chang, Molecular imaging of hydrogen peroxide produced for cell signaling, Nat. Chem. Biol. 3 (2007) 263–267, https://doi.org/10.1038/nchembio871.

[5] M. Sundaresan, Z.X. Yu, V.J. Ferrans, K. Irani, T. Finkel, Requirement for generation of H2O2 for platelet-derived growth factor signal transduction, Science 270 (1995) 296–299, https://doi.org/10.1126/science.270.5234.296.

[6] H. Sies, Role of metabolic H2O2 generation: redox signaling and oxidative stress, J. Biol. Chem. 289 (2014) 8735–8741, https://doi.org/10.1074/jbc.R113.544635.

[7] J.A. Bolduc, J.A. Collins, R.F. Loeser, Reactive oxygen species, aging and articular cartilage homeostasis, Free Radical Biol. Med. 132 (2019) 73–82, https://doi.org/10.1016/j.freeradbiomed.2018.08.038.

[8] S.I. Liochev, Reactive oxygen species and the free radical theory of aging, Free Radical Biol. Med. 60 (2013) 1–4, https://doi.org/10.1016/j.freeradbiomed.2013.02.011.

[9] W.-X. Wang, W.-L. Jiang, G.-J. Mao, M. Tan, J. Fei, Y. Li, C.-Y. Li, Monitoring the fluctuation of hydrogen peroxide in diabetes and its complications with a novel near-infrared fluorescent probe, Anal. Chem. 93 (2021) 3301–3307, https://doi.org/10.1021/acs.analchem.0c05364.

[10] S. Galadari, A. Rahman, S. Pallichankandy, F. Thayyullathil, Reactive oxygen species and cancer paradox: to promote or to suppress? Free Radical Biol. Med. 104 (2017) 144–164, https://doi.org/10.1016/j.freeradbiomed.2017.01.004.

[11] C. Chinopoulos, V. Adam-Vizi, Mitochondria deficient in complex I activity are depolarized by hydrogen peroxide in nerve terminals: relevance to Parkinson's disease, J. Neurochem. 76 (2001) 302–306, https://doi.org/10.1046/j.1471-4159.2001.00060.x.

[12] G.J. Harrison, L.R. Jordan, R.J. Willis, Deleterious effects of hydrogen peroxide on the function and ultrastructure of cardiac muscle and the coronary vasculature of perfused rat hearts, Can. J. Cardiol. 10 (1994) 843–849.

[13] N.G.N. Milton, Role of hydrogen peroxide in the aetiology of Alzheimer's disease: implications for treatment, Drugs Aging 21 (2004) 81–100, https://doi.org/10.2165/00002512-200421020-00002.

[14] Y.M. Lee, W. He, Y.-C. Liou, The redox language in neurodegenerative diseases: oxidative post-translational modifications by hydrogen peroxide, Cell Death Dis. 12 (2021) 58, https://doi.org/10.1038/s41419-020-03355-3.

[15] M.E. Abbas, W. Luo, L. Zhu, J. Zou, H. Tang, Fluorometric determination of hydrogen peroxide in milk by using a Fenton reaction system, Food Chem. 120 (2010) 327–331, https://doi.org/10.1016/j.foodchem.2009.10.024.

[16] S.B. Bankar, M.V. Bule, R.S. Singhal, L. Ananthanarayan, Glucose oxidase–an overview, Biotechnol. Adv. 27 (2009) 489–501, https://doi.org/10.1016/j.biotechadv.2009.04.003.

[17] M. Seki, K. Iida, M. Saito, H. Nakayama, S. Yoshida, Hydrogen peroxide production in Streptococcus pyogenes: involvement of lactate oxidase and coupling with aerobic utilization of lactate, J. Bacteriol. 186 (2004) 2046–2051, https://doi.org/10.1128/JB.186.7.2046-2051.2004.

[18] J. MacLachlan, A. Wotherspoon, R.O. Ansell, C. Brooks, Cholesterol oxidase: sources, physical properties and analytical applications, J. Steroid Biochem. Mol. Biol. 72 (2000) 169–195, https://doi.org/10.1016/S0960-0760(00)00044-3.

[19] J. Meier, E. M Hofferber, J. A Stapleton, N. M Iverson, Hydrogen peroxide sensors for biomedical applications, Chemosensors 7 (2019) 64, https://doi.org/10.3390/chemosensors7040064.

[20] L. Xing, W. Zhang, L. Fu, J.M. Lorenzo, Y. Hao, Fabrication and application of electrochemical sensor for analyzing hydrogen peroxide in food system and biological samples, Food Chem. 385 (2022) 132555, https://doi.org/10.1016/j.foodchem.2022.132555.

[21] Z. Li, Y. Jiang, C. Liu, Z. Wang, Z. Cao, Y. Yuan, M. Li, Y. Wang, D. Fang, Z. Guo, D. Wang, G. Zhang, J. Jiang, Emerging investigator series: dispersed transition metals on a nitrogen-doped carbon nanoframework for environmental hydrogen peroxide detection, Environ. Sci.: Nano 5 (2018) 1834–1843, https://doi.org/10.1039/C8EN00498F.

[22] F.S. Romolo, S. Connell, C. Ferrari, G. Suarez, J.-J. Sauvain, N.B. Hopf, Locating bomb factories by detecting hydrogen peroxide, Talanta 160 (2016) 15–20, https://doi.org/10.1016/j.talanta.2016.06.033.

[23] J.E. Giaretta, H. Duan, F. Oveissi, S. Farajikhah, F. Dehghani, S. Naficy, Flexible sensors for hydrogen peroxide detection: a critical review, ACS Appl. Mater. Interfaces 14 (2022) 20491–20505, https://doi.org/10.1021/acsami.1c24727.

[24] J.G. Mohanty, Jonathan S. Jaffe, Edward S. Schulman, Donald G. Raible, A highly sensitive fluorescent micro-assay of H_2O_2 release from activated human leukocytes using a dihydroxyphenoxazine derivative, J. Immunol. Methods (1997) 122–141. https://doi.org/10.1016/S0022-1759(96)00244-X.

[25] I. Sanz-Vicente, I. Rivero, L. Marcuello, M.P. Montano, S. de Marcos, J. Galbán, Portable colorimetric enzymatic disposable biosensor for histamine and simultaneous histamine/tyramine determination using a smartphone, Anal. Bioanal. Chem. 415 (2023) 1777–1786, https://doi.org/10.1007/s00216-023-04583-0.

[26] B. Zhao, F.A. Summers, R.P. Mason, Photooxidation of Amplex Red to resorufin: implications of exposing the Amplex Red assay to light, Free Radical Biol. Med. 53 (2012) 1080–1087, https://doi.org/10.1016/j.freeradbiomed.2012.06.034.

[27] N. Burmistrova, O. Kolontaeva, A. Duerkop, New nanomaterials and luminescent optical sensors for detection of hydrogen peroxide, Chemosensors 3 (2015) 253–273, https://doi.org/10.3390/chemosensors3040253.

[28] V. Sanz, S. de Marcos, J. Galbán, A reagentless optical biosensor based on the intrinsic absorption properties of peroxidase, Biosens. Bioelectron. 22 (2007) 956–964, https://doi.org/10.1016/j.bios.2006.04.008.

[29] D.-J. Zheng, Y.-S. Yang, H.-L. Zhu, Recent progress in the development of small-molecule fluorescent probes for the detection of hydrogen peroxide, TrAC, Trends Anal. Chem. 118 (2019) 625–651, https://doi.org/10.1016/j.trac.2019.06.031.

[30] J.-W. Chen, T.-C. Wu, W. Liang, J.-J. Ciou, C.-H. Lai, Boronates as hydrogen peroxide-reactive warheads in the design of detection probes, prodrugs, and nanomedicines used in tumors and other diseases, Drug Delivery Transl. Res. 13 (2023) 1305–1321, https://doi.org/10.1007/s13346-022-01248-w.

[31] E. Saxon, X. Peng, Recent advances in hydrogen peroxide responsive organoborons for biological and biomedical applications, Chembiochem 23 (2022) e202100366, https://doi.org/10.1002/cbic.202100366.

[32] L. Wang, X. Hou, H. Fang, X. Yang, Boronate-based fluorescent probes as a prominent tool for H2O2 sensing and recognition, Curr. Med. Chem. 29 (2022) 2476–2489, https://doi.org/10.2174/0929867328666210902101642.

[33] O.S. Wolfbeis, Probes, sensors, and labels: why is real progress slow? Angew. Chem. Int. Ed. 52 (2013) 9864–9865, https://doi.org/10.1002/anie.201305915.

[34] A. Hulanicki, S. Glab, F. Ingman, Chemical sensors: definitions and classification, Pure Appl. Chem. 63 (1991) 1247–1250, https://doi.org/10.1351/pac199163091247.

[35] Márta Vitai, László Góth, Reference ranges of normal blood catalase activity and levels in familial hypocatalasemia in Hungary, Clin. Chim. Acta 261 (1997) 35–42, https://doi.org/10.1016/S0009-8981(97)06514-5.

[36] M. Moßhammer, M. Kühl, K. Koren, Possibilities and challenges for quantitative optical sensing of hydrogen peroxide, Chemosensors 5 (2017) 28, https://doi.org/10.3390/chemosensors5040028.

[37] S. Ruan, W. Liu, W. Wang, Y. Lu, Research progress of SERS sensors based on hydrogen peroxide and related substances, Crit. Rev. Anal. Chem. (2023) 1–22, https://doi.org/10.1080/10408347.2023.2255901.

[38] K. Chattopadhyay, S. Mazumdar, Structural and conformational stability of horseradish peroxidase: effect of temperature and pH, Biochemistry 39 (2000) 263–270, https://doi.org/10.1021/bi990729o.

[39] S. Bocanegra-Rodríguez, N. Jornet-Martínez, C. Molins-Legua, P. Campíns-Falcó, New reusable solid biosensor with covalent immobilization of the horseradish peroxidase enzyme: in situ liberation studies of hydrogen peroxide by portable chemiluminescent determination, ACS Omega 5 (2020) 2419–2427, https://doi.org/10.1021/acsomega.9b03958.

[40] X.T. Zheng, Y. Zhong, H.E. Chu, Y. Yu, Y. Zhang, J.S. Chin, D.L. Becker, X. Su, X. J. Loh, Carbon dot-doped hydrogel sensor array for multiplexed colorimetric detection of wound healing, ACS Appl. Mater. Interfaces 15 (2023) 17675–17687, https://doi.org/10.1021/acsami.3c01185.

[41] X. Yang, C. Jin, J. Zheng, F. Chai, M. Tian, Portable intelligent paper-based sensors for rapid colorimetric and smartphone-assisted analysis of hydrogen peroxide for food, environmental and medical detection applications, Sens. Actuators, B 394 (2023) 134417, https://doi.org/10.1016/j.snb.2023.134417.

[42] R. Shen, P. Liu, Y. Zhang, Z. Yu, X. Chen, L. Zhou, B. Nie, A. Żaczek, J. Chen, J. Liu, Sensitive detection of single-cell secreted H_2O_2 by integrating a microfluidic droplet sensor and Au nanoclusters, Anal. Chem. 90 (2018) 4478–4484, https://doi.org/10.1021/acs.analchem.7b04798.

[43] M.-J. Lee, J.-A. Song, J.-H. Choi, J.-H. Shin, J.-W. Myeong, K.-P. Lee, T. Kim, K.-E. Park, B.-K. Oh, Horseradish peroxidase-encapsulated fluorescent bio-nanoparticle for ultra-sensitive and easy detection of hydrogen peroxide, Biosensors 13 (2023) 289, https://doi.org/10.3390/bios13020289.

[44] J. Goicoechea, P.J. Rivero, S. Sada, F.J. Arregui, Self-referenced optical fiber sensor for hydrogen peroxide detection based on LSPR of metallic nanoparticles in layer-by-layer films, Sensors 19 (2019), https://doi.org/10.3390/s19183872.

[45] O. Hosu, M. Lettieri, N. Papara, A. Ravalli, R. Sandulescu, C. Cristea, G. Marrazza, Colorimetric multienzymatic smart sensors for hydrogen peroxide, glucose and catechol screening analysis, Talanta 204 (2019) 525–532, https://doi.org/10.1016/j.talanta.2019.06.041.

[46] L.S. Lima, E.L. Rossini, L. Pezza, H.R. Pezza, Bioactive paper platform for detection of hydrogen peroxide in milk, Spectrochim. Acta, Part A 227 (2020) 117774, https://doi.org/10.1016/j.saa.2019.117774.

[47] Waris, A. Hasnat, S. Hasan, S. Bano, S. Sultana, A.O. Ibhadon, M.Z. Khan, Development of nanozyme based sensors as diagnostic tools in clinic applications: a review, J. Mater. Chem. B 11 (2023) 6762–6781, https://doi.org/10.1039/d3tb00451a.

[48] L. Tong, L. Wu, E. Su, Y. Li, N. Gu, Recent advances in the application of nanozymes in amperometric sensors: a review, Chemosensors 11 (2023) 233, https://doi.org/10.3390/chemosensors11040233.

[49] N.S. Heo, H.P. Song, S.M. Lee, H.-J. Cho, H.J. Kim, Y.S. Huh, M.I. Kim, Rosette-shaped graphitic carbon nitride acts as a peroxidase mimic in a wide pH range for fluorescence-based determination of glucose with glucose oxidase, Microchim. Acta 187 (2020) 286, https://doi.org/10.1007/s00604-020-04249-z.

[50] S. Zhuo, J. Fang, C. Zhu, J. Du, Preparation of palladium/carbon dot composites as efficient peroxidase mimics for H_2O_2 and glucose assay, Anal. Bioanal. Chem. 412 (2020) 963–972, https://doi.org/10.1007/s00216-019-02320-0.

[51] S. Zhang, Q. Pu, X. Deng, L. Zhang, N. Ye, Y. Xiang, A ratiometric fluorescence sensor for determination of choline based on gold nanoclusters and enzymatic reaction, Microchem. J. 187 (2023) 108402, https://doi.org/10.1016/j.microc.2023.108402.

[52] Y. Gao, Y. Wang, Y. Wang, P. Magaud, Y. Liu, F. Zeng, J. Yang, L. Baldas, Y. Song, Nanocatalysis meets microfluidics: a powerful platform for sensitive bioanalysis, TrAC, Trends Anal. Chem. 158 (2023) 116887, https://doi.org/10.1016/j.trac.2022.116887.

[53] P. Li, S. Zhang, C. Xu, L. Zhang, Q. Liu, S. Chu, S. Li, G. Mao, H. Wang, Coating Fe3O4 quantum dots with sodium alginate showing enhanced catalysis for capillary array-based rapid analysis of H_2O_2 in milk, Food Chem. 380 (2022) 132188, https://doi.org/10.1016/j.foodchem.2022.132188.

[54] T.T. Zhao, Z.W. Jiang, S.J. Zhen, C.Z. Huang, Y.F. Li, A copper(II)/cobalt(II) organic gel with enhanced peroxidase-like activity for fluorometric determination of hydrogen peroxide and glucose, Microchim. Acta 186 (2019) 168, https://doi.org/10.1007/s00604-019-3290-3.

[55] G. Li, Y. Chen, F. Liu, W. Bi, C. Wang, D. Lu, D. Wen, Portable visual and electrochemical detection of hydrogen peroxide release from living cells based on dual-functional Pt-Ni hydrogels, Microsyst. Nanoeng. 9 (2023) 152, https://doi.org/10.1038/s41378-023-00623-y.

[56] D. Calabria, A. Pace, E. Lazzarini, I. Trozzi, M. Zangheri, M. Guardigli, S. Pieraccini, S. Masiero, M. Mirasoli, Smartphone-based chemiluminescence glucose biosensor employing a peroxidase-mimicking, guanosine-based self-assembled hydrogel, Biosensors 13 (2023), https://doi.org/10.3390/bios13060650.

[57] Y. Mirzaei, A. Gholami, A. Sheini, M.M. Bordbar, An origami-based colorimetric sensor for detection of hydrogen peroxide and glucose using sericin capped silver nanoparticles, Sci. Rep. 13 (2023) 7064, https://doi.org/10.1038/s41598-023-34299-1.

[58] Y. Wei, J. Lu, Y. Xu, X. Song, Y. Yu, H. Zhang, X. Luo, Nanozyme-immobilized cellulose membranes designed by a simple hydrogen bond-dominated for colorimetric detection of hydrogen peroxide and uric acid, Microchem. J. 193 (2023) 109113, https://doi.org/10.1016/j.microc.2023.109113.

[59] M. Farooq, A. Hayat, M.H. Nawaz, M.S. Hassan, M. Nasir, H. Ajab, Tuning the structure and properties of MoS2-SrTiO3 nanocomposite and its enzyme mimic behavior for enhanced optical sensing and measurement of H_2O_2 in biological samples, Measurement 216 (2023) 112901, https://doi.org/10.1016/j.measurement.2023.112901.

[60] I. Ullah, A. Yaqub, M.Z.U. Haq, H. Ajab, A.T. Jafry, M.K. Khan, Sensitive and cost-effective colorimetric sensor based on enzyme mimic MoS_2@$CoTiO_3$ nanocomposite for detection of hydrogen peroxide in milk and tap water, J. Food Compos. Anal. 124 (2023) 105689, https://doi.org/10.1016/j.jfca.2023.105689.

[61] R. Bandi, M. Alle, C.-W. Park, S.-Y. Han, G.-J. Kwon, N.-H. Kim, J.-C. Kim, S.-H. Lee, Cellulose nanofibrils/carbon dots composite nanopapers for the smartphone-based colorimetric detection of hydrogen peroxide and glucose, Sens. Actuators, B 330 (2021) 129330, https://doi.org/10.1016/j.snb.2020.129330.

[62] Y. Li, X. Zhang, J. Shen, W. Qi, A colorimetric paper sensor based on self-assembled nanocomposite Pd−Pt@hemin-rGO/CNTs-COOH for the detection of H_2O_2, ChemNanoMat 9 (2023) e202200569, https://doi.org/10.1002/cnma.202200569.

[63] B. Peng, J. Xu, M. Fan, Y. Guo, Y. Ma, M. Zhou, Y. Fang, Smartphone colorimetric determination of hydrogen peroxide in real samples based on B, N, and S co-doped carbon dots probe, Anal. Bioanal. Chem. 412 (2020) 861–870, https://doi.org/10.1007/s00216-019-02284-1.

[64] M.-M. Liu, S.-H. Li, D.-D. Huang, Z.-W. Xu, Y.-W. Wu, Y. Lei, A.-L. Liu, MoOx quantum dots with peroxidase-like activity on microfluidic paper-based analytical device for rapid colorimetric detection of H2O2 released from PC12 cells, Sens. Actuators, B 305 (2020) 127512, https://doi.org/10.1016/j.snb.2019.127512.

[65] D. Cheng, J. Qin, Y. Feng, J. Wei, Synthesis of mesoporous CuO hollow sphere nanozyme for paper-based hydrogen peroxide sensor, Biosensors 11 (2021), https://doi.org/10.3390/bios11080258.

[66] S. Schnell, Validity of the Michaelis-Menten equation–steady-state or reactant stationary assumption: that is the question, FEBS J. 281 (2014) 464–472, https://doi.org/10.1111/febs.12564.

[67] S. Gu, S. Risse, Y. Lu, M. Ballauff, Mechanism of the oxidation of 3,3',5,5'-tetramethylbenzidine catalyzed by peroxidase-like Pt nanoparticles immobilized in spherical polyelectrolyte brushes: a kinetic study, ChemPhysChem 21 (2020) 450–458, https://doi.org/10.1002/cphc.201901087.

[68] A. Robert, B. Meunier, How to define a nanozyme, ACS Nano 16 (2022) 6956–6959, https://doi.org/10.1021/acsnano.2c02966.

[69] J. Huang, Y. Zheng, H. Niu, J. Huang, X. Zhang, J. Chen, B. Ma, C. Wu, Y. Cao, Y. Zhu, A multifunctional hydrogel for simultaneous visible H_2O_2 monitoring and accelerating diabetic wound healing, Adv. Healthcare Mater. (2023) e2302328, https://doi.org/10.1002/adhm.202302328.

[70] M. Mayer, S. Takegami, M. Neumeier, S. Rink, A. Jacobi von Wangelin, S. Schulte, M. Vollmer, A.G. Griesbeck, A. Duerkop, A.J. Baeumner, Electrochemiluminescence bioassays with a water-soluble luminol derivative can outperform fluorescence assays, Angew. Chem. Int. Ed. 57 (2018) 408–411, https://doi.org/10.1002/anie.201708630.

[71] S. Rink, A. Duerkop, A.J. Baeumner, Enhanced chemiluminescence of a superior luminol derivative provides sensitive smartphone-based point-of-care testing with enzymatic μPAD, Anal. Sens. (2023), https://doi.org/10.1002/anse.202200111.

[72] H. Vasconcelos, A. Matias, J. Mendes, J. Araújo, B. Dias, P.A. Jorge, C. Saraiva, J. M.M. de Almeida, L.C. Coelho, Compact biosensor system for the quantification of hydrogen peroxide in milk, Talanta 253 (2023) 124062, https://doi.org/10.1016/j.talanta.2022.124062.

[73] A. Schroter, T. Hirsch, Control of luminescence and interfacial properties as perspective for upconversion nanoparticles, Small (2023) e2306042, https://doi.org/10.1002/smll.202306042.

[74] G. Chen, H. Qiu, P.N. Prasad, X. Chen, Upconversion nanoparticles: design, nanochemistry, and applications in theranostics, Chem. Rev. 114 (2014) 5161–5214, https://doi.org/10.1021/cr400425h.

[75] X. Wang, J. Fu, C. Jiang, X. Liao, Y. Chen, T. Jia, G. Chen, X. Feng, Specific and long-term luminescent monitoring of hydrogen peroxide in tumor metastasis, Adv. Mater. 35 (2023) e2210948, https://doi.org/10.1002/adma.202210948.

[76] Y. Wu, Da Lei, J. Li, Y. Luo, Y. Du, S. Zhang, B. Zu, Y. Su, X. Dou, Controlled synthesis of preferential facet-exposed Fe-MOFs for ultrasensitive detection of peroxides, Small (2024) e2401024, https://doi.org/10.1002/smll.202401024.

[77] A. Dutta, U. Maitra, Naked-eye detection of hydrogen peroxide on photoluminescent paper discs, ACS Sens. 7 (2022) 513–522, https://doi.org/10.1021/acssensors.1c02322.

[78] Q. Chen, L. Yang, K. Guo, J. Yang, J.-M. Han, Expedite fluorescent sensor prototype for hydrogen peroxide detection with long-life test substrates, ACS Omega 6 (2021) 11447–11457, https://doi.org/10.1021/acsomega.1c00471.

[79] Y. Zhang, Y. Feng, Z. Zhang, M. Zhang, Highly efficient fluorescent film probe of hydrogen peroxide vapor, Microchem. J. 158 (2020) 105290, https://doi.org/10.1016/j.microc.2020.105290.

[80] Z. Xu, C. Zeng, Y. Zhao, M. Zhou, T. Lv, C. Song, T. Qin, L. Wang, B. Liu, X. Peng, Smartphone-based on-site detection of hydrogen peroxide in milk by using a portable ratiometric fluorescent probe, Food Chem. 410 (2023) 135381, https://doi.org/10.1016/j.foodchem.2022.135381.

[81] J. Chang, H. Li, T. Hou, W. Duan, F. Li, Paper-based fluorescent sensor via aggregation induced emission fluorogen for facile and sensitive visual detection of hydrogen peroxide and glucose, Biosens. Bioelectron. 104 (2018) 152–157, https://doi.org/10.1016/j.bios.2018.01.007.

[82] H. Mei, Y. Ma, H. Wu, X. Wang, Fluorescent and visual assay of H_2O_2 and glucose based on a highly sensitive copper nanoclusters-Ce(III) fluoroprobe, Anal. Bioanal. Chem. 413 (2021) 2135–2146, https://doi.org/10.1007/s00216-021-03181-2.

[83] C. Meng, F. Du, A. Abdussalam, A. Wang, D. Snizhko, W. Zhang, G. Xu, Sonochemiluminescence using apertureless USB piezoelectric ultrasonic transducer and its applications for the detection of hydrogen peroxide, glucose, and glucose oxidase activity, Anal. Chem. 93 (2021) 14934–14939, https://doi.org/10.1021/acs.analchem.1c03834.

[84] L. Sharma, S. Gouraj, P. Raut, C. Tagad, Development of a surface-modified paper-based colorimetric sensor using synthesized Ag NPs-alginate composite, Environ. Technol. 42 (2021) 3441–3450, https://doi.org/10.1080/09593330.2020.1732471.

[85] Z. He, J. Huang, W. Shen, X. Lei, Y. Zhang, L. Zhu, X. Shen, D. Zhang, D. Yu, M. Zhou, A paper-based fluorescent sensor for rapid early screening of oral squamous cell carcinoma, ACS Appl. Mater. Interfaces 15 (2023) 24913–24922, https://doi.org/10.1021/acsami.3c03545.

[86] J. Noh, M. Jung, Y. Jung, C. Yeom, M. Pyo, G. Cho, Key issues with printed flexible thin film transistors and their application in disposable RF sensors, Proc. IEEE 103 (2015) 554–566, https://doi.org/10.1109/JPROC.2015.2410303.

[87] D. Mampallil, H.B. Eral, A review on suppression and utilization of the coffee-ring effect, Adv. Colloid Interface Sci. 252 (2018) 38–54, https://doi.org/10.1016/j.cis.2017.12.008.

[88] Y. Shen, Y. Wei, C. Zhu, J. Cao, D.-M. Han, Ratiometric fluorescent signals-driven smartphone-based portable sensors for onsite visual detection of food contaminants, Coord. Chem. Rev. 458 (2022) 214442, https://doi.org/10.1016/j.ccr.2022.214442.

[89] D. Zhang, Q. Liu, Biosensors and bioelectronics on smartphone for portable biochemical detection, Biosens. Bioelectron. 75 (2016) 273–284, https://doi.org/10.1016/j.bios.2015.08.037.

[90] G. Ross, Y. Zhao, A.J. Bosman, A. Geballa-Koukoula, H. Zhou, C.T. Elliott, M. Nielen, K. Rafferty, G. Salentijn, Best practices and current implementation of emerging smartphone-based (bio)sensors – Part 1: data handling and ethics, TrAC, Trends Anal. Chem. 158 (2023) 116863, https://doi.org/10.1016/j.trac.2022.116863.

[91] P. Rai, S. Verma, S. Mehrotra, S.K. Sharma, A QR code-integrated chromogenic paper strip for detection of hydrogen peroxide in aqueous samples, Anal. Methods 15 (2023) 5286–5293, https://doi.org/10.1039/d3ay01584j.

[92] R. Meng, Z. Yu, Q. Fu, Y. Fan, L. Fu, Z. Ding, S. Yang, Z. Cao, L. Jia, Smartphone-based colorimetric detection platform using color correction algorithms to reduce external interference, Spectrochim. Acta, Part A 316 (2024) 124350, https://doi.org/10.1016/j.saa.2024.124350.

[93] V. Doğan, E. Yüzer, V. Kılıç, M. Şen, Non-enzymatic colorimetric detection of hydrogen peroxide using a μPAD coupled with a machine learning-based smartphone app, Analyst 146 (2021) 7336–7344, https://doi.org/10.1039/d1an01888d.

[94] P. Cebrián, L. Pérez-Sienes, I. Sanz-Vicente, Á. López-Molinero, S. de Marcos, J. Galbán, Solving color reproducibility between digital devices: a robust approach of smartphones color management for chemical (Bio)Sensors, Biosensors 12 (2022), https://doi.org/10.3390/bios12050341.

[95] A. García, M.M. Erenas, E.D. Marinetto, C.A. Abad, I. de Orbe-Paya, A.J. Palma, L. F. Capitán-Vallvey, Mobile phone platform as portable chemical analyzer, Sens. Actuators, B 156 (2011) 350–359, https://doi.org/10.1016/j.snb.2011.04.045.

[96] J. Schindelin, I. Arganda-Carreras, E. Frise, V. Kaynig, M. Longair, T. Pietzsch, S. Preibisch, C. Rueden, S. Saalfeld, B. Schmid, J.-Y. Tinevez, D.J. White, V. Hartenstein, K. Eliceiri, P. Tomancak, A. Cardona, Fiji: an open-source platform for biological-image analysis, Nat. Methods 9 (2012) 676–682, https://doi.org/10.1038/nmeth.2019.

[97] N.Y. Tiuftiakov, A.V. Kalinichev, N.V. Pokhvishcheva, M.A. Peshkova, Digital color analysis for colorimetric signal processing: towards an analytically justified choice of acquisition technique and color space, Sens. Actuators, B 344 (2021) 130274, https://doi.org/10.1016/j.snb.2021.130274.

[98] Y. Zhang, Y. Wu, Y. Zhang, A. Ozcan, Color calibration and fusion of lens-free and mobile-phone microscopy images for high-resolution and accurate color reproduction, Sci. Rep. 6 (2016) 27811, https://doi.org/10.1038/srep27811.

[99] A. Skandarajah, C.D. Reber, N.A. Switz, D.A. Fletcher, Quantitative imaging with a mobile phone microscope, PLoS One 9 (2014) e96906, https://doi.org/10.1371/journal.pone.0096906.

[100] M. Moßhammer, M. Kühl, K. Koren, Possibilities and challenges for quantitative optical sensing of hydrogen peroxide, Chemosensors 5 (2017) 28, https://doi.org/10.3390/chemosensors5040028.

[101] K. Koren, C.M. McGraw, Let's talk about slime; or why biofouling needs more attention in sensor science, ACS Sens. 8 (2023) 2432–2439, https://doi.org/10.1021/acssensors.3c00961.

[102] M. Moßhammer, V. Schrameyer, P.Ø. Jensen, K. Koren, M. Kühl, Extracellular hydrogen peroxide measurements using a flow injection system in combination with microdialysis probes - potential and challenges, Free Radical Biol. Med. 128 (2018) 111–123, https://doi.org/10.1016/j.freeradbiomed.2018.05.089.

[103] M. Moßhammer, K. Koren, M. Kühl, Flow Injection Analysis with Microdialysis Probes Enable Minimally Invasive and Dynamic H_2O_2 Measurements, Proceedings 2 (2018) 992, in: https://doi.org/10.3390/proceedings2130992.

[104] F. Li, J. Liu, L. Guo, J. Wang, K. Zhang, J. He, H. Cui, High-resolution temporally resolved chemiluminescence based on double-layered 3D microfluidic paper-based device for multiplexed analysis, Biosens. Bioelectron. 141 (2019) 111472, https://doi.org/10.1016/j.bios.2019.111472.

[105] S. Yuan, R. Yu, Y. Tu, Y. Du, X. Feng, F. Nie, An enhanced chemiluminescence hybrids of luminol by sulfonated polyaniline decorated copper-based metal organic frame composite applicable to the measurement of hydrogen peroxide in a wide pH range, Talanta 254 (2023) 124183, https://doi.org/10.1016/j.talanta.2022.124183.

[106] C.-L. Shen, G.-S. Zheng, M.-Y. Wu, J.-Y. Wei, Q. Lou, Y.-L. Ye, Z.-Y. Liu, J.-H. Zang, L. Dong, C.-X. Shan, Chemiluminescent carbon nanodots as sensors for hydrogen peroxide and glucose, Nanophotonics 9 (2020) 3597–3604, https://doi.org/10.1515/nanoph-2020-0233.

[107] T. Sun, Y. Su, M. Sun, Y. Lv, Homologous chemiluminescence resonance energy transfer on the interface of WS2 quantum dots for monitoring photocatalytic H_2O_2 evaluation, Microchem. J. 168 (2021) 106344, https://doi.org/10.1016/j.microc.2021.106344.

[108] R. Gaikwad, P.R. Thangaraj, A.K. Sen, Direct and rapid measurement of hydrogen peroxide in human blood using a microfluidic device, Sci. Rep. 11 (2021) 2960, https://doi.org/10.1038/s41598-021-82623-4.

[109] Y. Malyukin, V. Seminko, P. Maksimchuk, E. Okrushko, O. Sedyh, Y. Zorenko, Hydrogen peroxide sensing using Ce^{3+} luminescence of cerium oxide (CeO_2-x) nanoparticles, Opt. Mater. 85 (2018) 303–307, https://doi.org/10.1016/j.optmat.2018.08.063.

[110] V. Seminko, P. Maksimchuk, V. Klochkov, Y. Neuhodov, L. Demchenko, S. Yefimova, Reversible CeO_{2-x} and CeO_{2-x}:Eu^{3+} luminescent hydrogen peroxide sensors with recovery rates controlled by temperature and UV irradiation, J. Phys. Chem. C 127 (2023) 10662–10669, https://doi.org/10.1021/acs.jpcc.3c02637.

[111] P. Virbickas, G. Kavaliauskaitė, A. Valiūnienė, V. Plaušinaitienė, A.I. Rekertaitė, A. Ramanavičius, Cobalt hexacyanoferrate based optical sensor for continuous optical sensing of hydrogen peroxide, Electrochim. Acta 362 (2020) 137202, https://doi.org/10.1016/j.electacta.2020.137202.

[112] H.D. Duong, J.I. Rhee, Development of ratiometric fluorescence sensors based on CdSe/ZnS quantum dots for the detection of hydrogen peroxide, Sensors 19 (2019), https://doi.org/10.3390/s19224977.

[113] C. Liu, F. Hu, W. Yang, J. Xu, Y. Chen, A critical review of advances in surface plasmon resonance imaging sensitivity, TrAC, Trends Anal. Chem. 97 (2017) 354–362, https://doi.org/10.1016/j.trac.2017.10.001.

[114] V. Semwal, B.D. Gupta, Highly selective SPR based fiber optic sensor for the detection of hydrogen peroxide, Sens. Actuators, B 329 (2021) 129062, https://doi.org/10.1016/j.snb.2020.129062.

[115] H.E. Posch, O.S. Wolfbeis, Optical sensor for hydrogen peroxide, Microchim. Acta 97 (1989) 41–50, https://doi.org/10.1007/BF01197282.

[116] X. Wang, O.S. Wolfbeis, Optical methods for sensing and imaging oxygen: materials, spectroscopies and applications, Chem. Soc. Rev. 43 (2014) 3666–3761, https://doi.org/10.1039/C4CS00039K.

[117] L. Ding, S. Chen, W. Zhang, Y. Zhang, X. Wang, Fully reversible optical sensor for hydrogen peroxide with fast response, Anal. Chem. 90 (2018) 7544–7551, https://doi.org/10.1021/acs.analchem.8b01159.

[118] A.Ø. Tjell, B. Jud, R. Schaller-Ammann, T. Mayr, Optical hydrogen peroxide sensor for measurements in flow, Sens. Actuators, B (2023) 134904, https://doi.org/10.1016/j.snb.2023.134904.

[119] A.Ø. Tjell, L.-E. Meyer, B. Jud, S. Kara, T. Mayr, At-line monitoring of hydrogen peroxide released from its photocatalytic and continuous synthesis, React. Chem. Eng. 9 (2024) 777–781, https://doi.org/10.1039/D3RE00659J.

[120] S. Fuchs, V. Rieger, A.Ø. Tjell, S. Spitz, K. Brandauer, R. Schaller-Ammann, J. Feiel, P. Ertl, I. Klimant, T. Mayr, Optical glucose sensor for microfluidic cell culture systems, Biosens. Bioelectron. 237 (2023) 115491, https://doi.org/10.1016/j.bios.2023.115491.

[121] P.M. Nowak, R. Wietecha-Posłuszny, J. Pawliszyn, White analytical chemistry: an approach to reconcile the principles of green analytical chemistry and functionality, TrAC, Trends Anal. Chem. 138 (2021) 116223, https://doi.org/10.1016/j.trac.2021.116223.

[122] M. Buzdar, A. Yaqub, A. Hayat, M.Z. Ul Haq, A. Khan, H. Ajab, Paper based colorimetric sensor using novel green magnetized nanocomposite of pinus for hydrogen peroxide detection in water and milk, Food Biosci. 55 (2023) 103014, https://doi.org/10.1016/j.fbio.2023.103014.

[123] S. Vijayaram, H. Razafindralambo, Y.-Z. Sun, S. Vasantharaj, H. Ghafarifarsani, S. H. Hoseinifar, M. Raeeszadeh, Applications of green synthesized metal nanoparticles - a review, Biol. Trace Elem. Res. (2023) 1–27, https://doi.org/10.1007/s12011-023-03645-9.

[124] Le Dong, R. Li, L. Wang, X. Lan, H. Sun, Y. Zhao, L. Wang, Green synthesis of platinum nanoclusters using lentinan for sensitively colorimetric detection of glucose, Int. J. Biol. Macromol. 172 (2021) 289–298, https://doi.org/10.1016/j.ijbiomac.2021.01.049.

[125] J. Seemann, F.-R. Rapp, A. Zell, G. Gauglitz, Classical and modern algorithms for the evaluation of data from sensor-arrays, Fresenius' J. Anal. Chem. 359 (1997) 100–106. https://doi.org/10.1007/s002160050543.

[126] W. Yu, X. Zheng, M. Tan, J. Wang, B. Wu, J. Ma, Y. Pan, B. Chen, C. Chu, Field quantification of hydroxyl radicals by flow-injection chemiluminescence analysis with a portable device, Envirom. Sci. Technol. 58 (2024) 2808–2816, https://doi.org/10.1021/acs.est.3c09140.